JOURNAL OF PETROLOGY | VOLUME 39 | NUMBER 5 | PAGES 973–994 | 1998

# Geochemical Characteristics of the Youngest Volcano (Mount Ross) in the Kerguelen Archipelago: Inferences for Magma Flux, Lithosphere Assimilation and Composition of the Kerguelen Plume

**D. WEIS[1]*, F. A. FREY[2], A. GIRET[3] AND J.-M. CANTAGREL[4]**

[1]DÉPARTEMENT DES SCIENCES DE LA TERRE ET DE L'ENVIRONNEMENT, UNIVERSITÉ LIBRE DE BRUXELLES, CP 160/02, AVE. F.D. ROOSEVELT 50, B-1050 BRUSSELS, BELGIUM

[2]DEPARTMENT OF EARTH, ATMOSPHERIC AND PLANETARY SCIENCES, MASSACHUSETTS INSTITUTE OF TECHNOLOGY, CAMBRIDGE, MA 02139, USA

[3]UNIVERSITÉ JEAN MONNET, FACULTÉ DES SCIENCES, DÉPARTEMENT DE GÉOLOGIE–PÉTROLOGIE–GÉOCHIMIE, CNRS–UMR 6524, 23 RUE DU DOCTEUR PAUL MICHELON, 42023 SAINT-ETIENNE, CEDEX 2, FRANCE

[4]UNIVERSITÉ DE CLERMONT-FERRAND, CNRS-UA 10, 5, RUE KESSLER, 63000 CLERMONT-FERRAND, FRANCE

**RECEIVED SEPTEMBER 10, 1997; REVISED TYPESCRIPT ACCEPTED DECEMBER 2, 1997**

*Mount Ross is the youngest, ~1–0·1 Ma, volcanic edifice recognized in the Kerguelen Archipelago, which is located on the northern part of the submarine Kerguelen Plateau. Lava types range from basaltic trachyandesite to trachyte and extensive glaciation has exposed an intrusive core ranging from gabbro to syenite. Mount Ross rocks are not as silica undersaturated as the basanite to phonolite Upper Miocene lavas erupted in the Southeast Province of the archipelago; however, both lava suites are characterized by relatively high $^{87}Sr/^{86}Sr$ (0·7051–0·7054 and 0·7054–0·7058, respectively) and low $^{206}Pb/^{204}Pb$ (18·02–18·14 and 18·06–18·27, respectively). The abundant trachytes and phonolites in the age range from Lower Miocene to Pleistocene on the Kerguelen Archipelago indicate that the supply of basaltic magma has been low for the last 20 my. Despite the prolonged time period required for extensive mineral fractionation, there is no evidence for assimilation of geochemically distinctive lithosphere; i.e. most of the trachytes and syenites have initial isotopic ratios within the narrow range of the more mafic rocks. Volcanic and plutonic rocks of diverse composition and age (~0·1–30 Ma) in the Kerguelen Archipelago have similar initial isotopic ratios; consequently, we infer that the Kerguelen plume is characterized by $^{87}Sr/^{86}Sr$ = 0·7051–0·7058, $^{143}Nd/^{144}Nd$ = 0·51263–0·51249 and $^{206}Pb/^{204}Pb$ = 18·02–18·27.*

KEY WORDS: *geochemistry; isotopes; Kerguelen Islands; magma flux; plume magmatism*

## INTRODUCTION

The Kerguelen Archipelago on the northern Kerguelen Plateau (Fig. 1a) has a history from ~40 to 0·1 Ma of volcanism that is attributed to the Kerguelen plume (Weis *et al.*, 1989*b*). Before forming the Kerguelen Archipelago and perhaps Heard Island which are on the Antarctic plate, the long-lived (~115 my) Kerguelen plume formed a very large igneous province (Kerguelen Plateau) followed by an ~5000 km hotspot track (Ninetyeast Ridge, Weis *et al.*, 1992). The plume is geochemically distinctive because it has DUPAL isotopic characteristics (Weis *et al.*, 1989*b*). Weis *et al.* (1993) proposed that the purest representation of the Sr, Nd and Pb isotopic characteristics of this plume are in the Upper Miocene lavas erupted from 10·2 to 6·6 Ma in the Southeast Province of the archipelago. In contrast to the conclusion of Weis

*Corresponding author. e-mail: dweis@ulb.ac.be

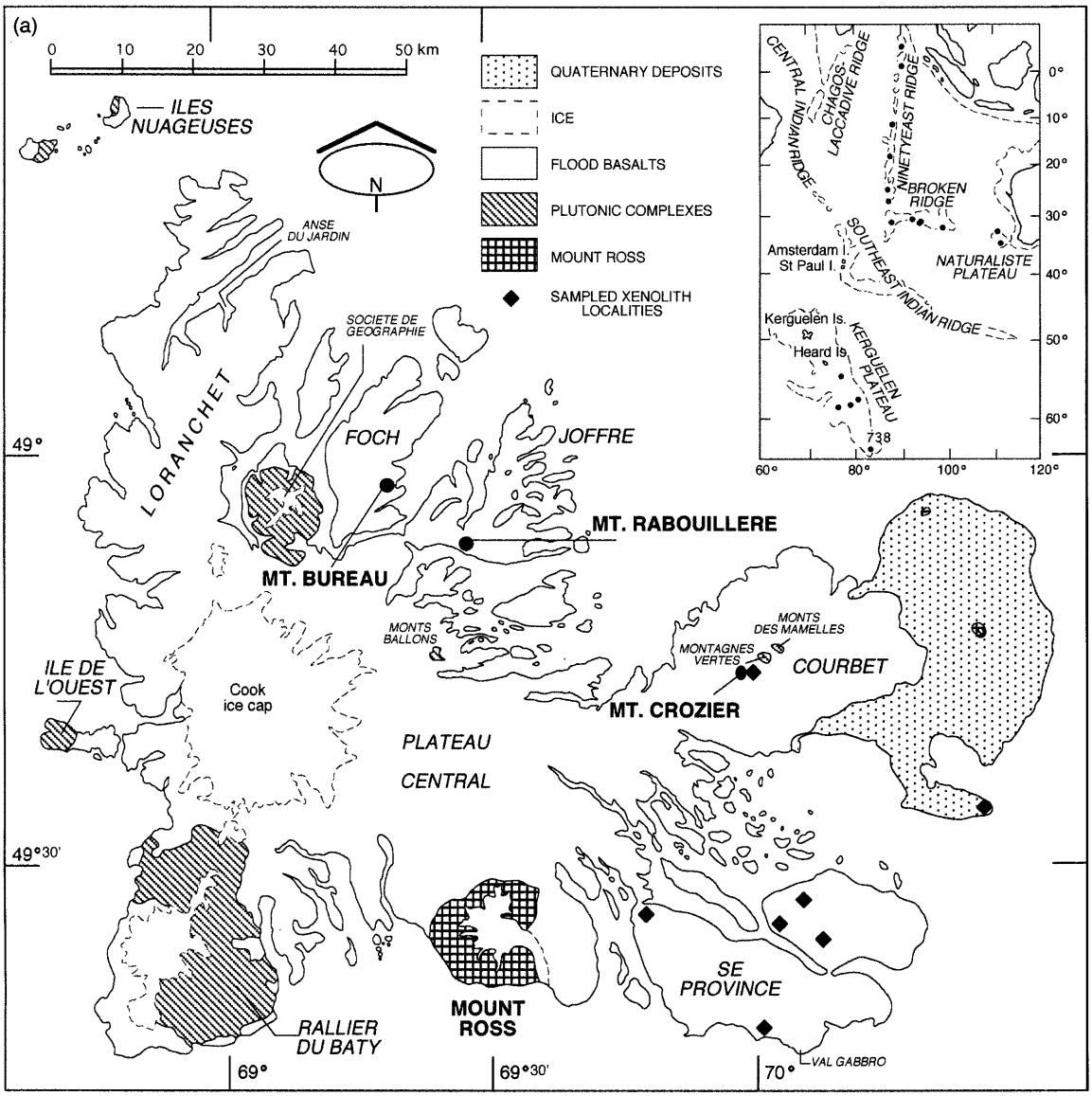


**Fig. 1.**

*et al.* (1993), Class *et al.* (1993) proposed that some recently erupted Heard Island lavas are the purest representation of the Kerguelen plume. The pros and cons of these different interpretations were discussed by Class *et al.* (1996) and Frey & Weis (1995, 1996). In an effort to further evaluate these hypotheses and to identify the petrogenetic processes that were important in constructing the archipelago, we are determining the spatial and temporal geochemical variations in archipelago lavas. In this paper we discuss the igneous rocks associated with Mount Ross, one of the youngest (<1 Ma) and largest volcanic edifices in the Kerguelen archipelago; at 1850 m it forms the highest summit (Fig. 1).

Highly evolved lavas, trachytes, are abundant at Mount Ross. We conclude that fractional crystallization of a more mafic magma within the crust was a major process in creating these trachytes. During this period of crustal processing assimilation of lithosphere was likely. However, the geochemical characteristics of Mount Ross trachytes provide meagre evidence for assimilation of a geochemically distinctive lithosphere component. In contrast, the relatively high $^{87}Sr/^{86}Sr$ (up to 0·7079) in some trachytes from Heard Island, which is located ~400 km further south on the Kerguelen Plateau (Fig. 1a), may indicate assimilation of a lithospheric component (Barling *et al.*, 1994). The contrasting inferences from

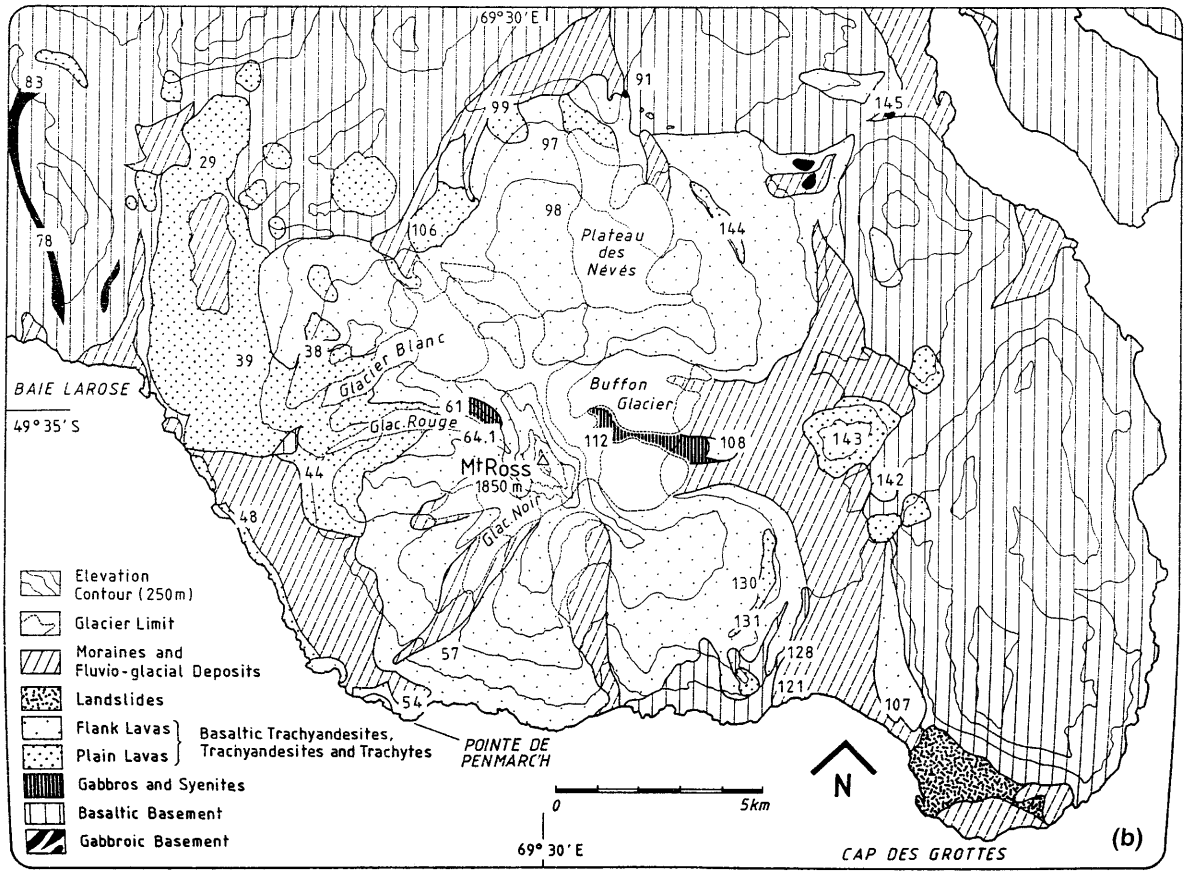


**Fig. 1.** (a) Generalized geological map of the Kerguelen Archipelago showing the locations of Mount Ross and the Southeast Province and the major features on the Archipelago. Lavas from sections of the flood basalts at Mt Bureau and Mt Rabouillère were studied by Yang *et al.* (1998) and at Mt Crozier by Damasceno *et al.* (1997). Inset: map of the eastern Indian Ocean showing major volcanic structures that are attributed to the Kerguelen plume, i.e. the ~115–85 Ma Kerguelen Plateau and Broken Ridge, the ~82–38 Ma Ninetyeast Ridge and the ~40–0·1 Ma Kerguelen Archipelago located at ~50°S on the northern Kerguelen Plateau. ●, locations where basaltic basement has been recovered by dredging and drilling. (b) Simplified geological map of Mount Ross showing major units and sample locations.

these two islands may reflect the absence of geochemically distinctive Cretaceous lithosphere beneath the Kerguelen Archipelago (Coffin & Eldholm, 1994).

## GEOLOGY OF MOUNT ROSS

Mount Ross was constructed on flood basalts that cover ~85% of the archipelago (Fig. 1a). These flood basalts are cut by numerous dikes and sills of gabbros which are older than 20 Ma (Giret & Lameyre, 1983; Giret & Beaux, 1984; Giret *et al.*, 1988). Seismic refraction data in the vicinity of Mount Ross indicate an upper crust of ~11 km ($V_p$ = 5·35–6·60 km/s) and a lower crust of 6–7 km ($V_p$ = 6·85–7·35 km/s). Although the total crustal thickness is typical of the archipelago, the seismic velocity ($V_p$) in the upper crust at Mount Ross exceeds those of the surrounding flood basalts (Recq *et al.*, 1994).

Giret *et al.* (1988) summarized the morphological characteristics of Mount Ross volcano. It is a nearly circular cone with very steep slopes, a diameter of 16 km, a preserved area of 195 km$^2$, a volume of 135 km$^3$ and a central depression, 4·5 km in diameter (Fig. 1b). At ~1000 m below the summit, the regression of several glaciers in a radial system of valleys has exposed the volcanic and plutonic rocks forming the interior of the volcano. The volcano flanks are made of flows of trachyandesite and basaltic trachyandesite [nomenclature of Le Bas *et al.* (1986)] interbedded with pyroclastic deposits and thick trachytic flows. The summit area is a 1 km pile of pyroclastic deposits intruded by dikes and sills of trachytes. Trachyte also occurs as small peripheral

cones and tabular structures filling >100 m depressions. Some of the lavas contain xenoliths of gabbro and monzonite; an intrusive complex of gabbro, monzonite and rare nepheline syenite with numerous trachytic dikes is exposed high on the flanks (Fig. 1b). Although on the basis of previous age considerations (Nougier, 1970), Giret *et al.* (1988) proposed that Mount Ross was formed in two stages, a basaltic phase at 4–2 Ma followed by a trachytic stage at <0·5 Ma, new K/Ar ages indicate that most of the Mount Ross plutonic and volcanic rocks are young, <1 Ma.

## SAMPLING

Although modest in height, extreme weather conditions, abundant ice and its remote location make access to Mount Ross difficult. Our samples are from glacial valleys, the volcano flanks and surrounding basement. Sample locations are shown in Fig. 1b. We selected for geochemical studies five samples of the 20–25 Ma basement rocks (four gabbros and a flood basalt), and 22 samples from Mount Ross [two gabbros, two syenites, seven lavas with 2·3–4% MgO (lavas with higher MgO contents were not found), and 11 highly evolved lavas (0·16–1·9% MgO)]. In addition, Nougier (1970) reported major element compositions of 22 Mount Ross trachytes.

## ANALYTICAL PROCEDURES

Abundances of major elements and the trace elements Rb, Sr, Ba, V, Ni, Zn, Ga, Y, Zr and Nb (Table 1) were determined by X-ray fluorescence (XRF) at the University of Massachusetts, Amherst (Rhodes, 1983). All XRF data are means of duplicate analyses. Abundances of the trace elements, Sc, Cr, Co, Hf, Ta, Th, and several rare earth elements (REE) (Table 1) were determined by instrumental neutron activation at MIT (Ila & Frey, 1984). Precision estimates are indicated by duplicate analyses for eight samples (Table 1b).

Samples for K–Ar dating were selected according to their structural location and their mineralogy. In particular, the zeolitized basement is best dated by using the relatively unaltered intrusive gabbroic dikes. Classical K–Ar analytical procedures (Cantagrel & Baubron, 1983) were used on whole-rock samples after separation of olivine and pyroxene phenocrysts. Argon was extracted from sample aliquots of 0·5–2 g and analyzed by isotopic dilution with a modified MS10 mass spectrometer. Potassium abundance was determined in duplicate by atomic absorption spectrometry (Table 2). Errors in age are $\pm 2$ SD (Table 2).

Samples for radiogenic isotope analyses (Sr, Nd and Pb) were selected to include samples from all parts of the volcano and to encompass the entire range of chemical composition (Table 3). The chemical procedure used is similar to that described in Weis *et al.* (1987) with improvements discussed in Weis & Frey (1991). The samples are not visibly altered and tests indicated that acid leaching had no effect on $^{87}Sr/^{86}Sr$ ratios. Therefore, Mount Ross samples were not acid leached.

Total blank values were <1 ng for all three isotopic systems considered. Such values are negligible in view of the elemental concentrations in the samples. Sr and Nd isotopic compositions were measured, on single Ta filaments and triple Re–Ta filaments, respectively, in the dynamic mode, on a VG Sector 54 multicollector mass spectrometer with an internal precision better than $1 \times 10^{-5}$ unless specified in Table 3. Sr isotopic ratios were normalized to $^{86}Sr/^{88}Sr = 0{\cdot}1194$ and Nd isotopic ratios (147, 146, 145, 144, 143 and 142), measured as metal, to $^{146}Nd/^{144}Nd = 0{\cdot}7219$. The average $^{87}Sr/^{86}Sr$ value of the NBS 987 Sr standard was $0{\cdot}710232 \pm 8$ ($2\sigma_m$ on 18 samples) and analyses of the Merck Nd standard yielded $^{143}Nd/^{144}Nd = 0{\cdot}51173 \pm 1$ and $^{145}Nd/^{144}Nd = 0{\cdot}348417 \pm 5$ ($2\sigma_m$ on 12 samples). Pb isotopic compositions and Pb and U concentrations by isotope dilution were measured on single Re filaments with a Finnigan Mat 260 mass spectrometer, using the $H_3PO_4$–silica gel technique. All Pb isotopic ratios were corrected for mass fractionation ($0{\cdot}13 \pm 0{\cdot}04\%$ per a.m.u.) on the basis of 72 analyses of the NBS 981 Pb standard for a temperature range between 1090°C and 1200°C. Between-run precisions were better than ~0·1% for $^{206}Pb/^{204}Pb$ and $^{207}Pb/^{204}Pb$ and better than ~0·15% for $^{208}Pb/^{204}Pb$.

## PETROGRAPHY

The volcanic and plutonic rocks from Mount Ross have similar mineralogy. Gabbros typically have a doleritic texture with pyroxene and minor olivine surrounded by plagioclase either as microlites or coarse crystals with accessory apatite, Fe–Ti oxides and rare biotite. The basaltic trachyandesites and trachyandesites typically have a fluidal texture. They contain abundant plagioclase ($An_{50–80}$), augite and olivine ($Fo_{63–80}$) as phenocrysts and groundmass phases; in some cases the groundmass also contains abundant Fe–Ti oxides. The thick and obviously viscous trachyte flows have a groundmass of fluidal plagioclase and potassium feldspar microlites surrounding abundant phenocrysts of plagioclase, potassium feldspar, augite and minor hedenbergite. Acmitic augite is an interstitial phase and rare biotite is largely replaced by Fe–Ti oxides. Angular, 1–10 cm, xenoliths of basalt and gabbro are most common in the margins of trachyte flows. There is a progressive transition from trachyte to

*Table 1a: Compositional data for ~20–25 Ma basement rocks in the Mount Ross area (major elements in wt %; trace elements in ppm)*

| Sample: | 145 | 83 | 78 | 91 | 128 |
|---|---|---|---|---|---|
| Rock type: | G | G | G | G | TB |
| $SiO_2$ | 47·71 | 49·71 | 51·50 | 51·14 | 48·46 |
| $TiO_2$ | 1·75 | 1·66 | 2·48 | 2·45 | 2·82 |
| $Al_2O_3$ | 16·31 | 15·96 | 15·48 | 17·27 | 17·40 |
| $Fe_2O_3$ | 11·43 | 11·04 | 10·14 | 9·41 | 11·63 |
| MnO | 0·17 | 0·15 | 0·14 | 0·12 | 0·17 |
| MgO | 7·32 | 6·39 | 6·27 | 4·29 | 4·02 |
| CaO | 10·92 | 10·44 | 9·44 | 6·91 | 9·75 |
| $Na_2O$ | 2·95 | 3·23 | 3·04 | 4·77 | 3·47 |
| $K_2O$ | 0·80 | 0·96 | 1·10 | 2·66 | 1·66 |
| $P_2O_5$ | 0·22 | 0·23 | 0·32 | 0·63 | 0·71 |
| Total | 99·59 | 99·76 | 99·89 | 99·65 | 100·08 |
| Rb | | | | | 36·9 |
| Cs | | | | | 0·28 |
| Sr | | | | | 756 |
| Ba | | | | | 753 |
| Sc | 29·0 | 25·4 | 19·9 | 14·1 | 19·7 |
| V | | | | | 178 |
| Cr | 218 | 246 | 154 | 6·0 | 55 |
| Co | 41·2 | 43·1 | 40·2 | 28·2 | 34·2 |
| Ni | | | | | 44 |
| Zn | | | | | 94 |
| Ga | | | | | 21·5 |
| Y | | | | | 24·4 |
| Zr | | | | | 220 |
| Nb | | | | | 34 |
| Hf | 2·79 | 3·00 | 3·07 | 6·24 | 5·09 |
| Ta | 0·88 | 0·93 | 1·55 | 2·54 | 1·97 |
| Th | 1·58 | 1·75 | 2·01 | 5·36 | 3·9 |
| U | 0·37 | 0·48 | 0·46 | 1·20 | 0·84 |
| Pb | 1·6 | 1·4 | 1·9 | 5·4 | 2·8 |
| La | 15·5 | 15·5 | 21·1 | 45·1 | 36·2 |
| Ce | 34·7 | 35·5 | 47·4 | 96·5 | 84·3 |
| Nd | 17·5 | 18·9 | 22·1 | 40·0 | 40·1 |
| Sm | 3·56 | 4·57 | 5·01 | 7·76 | 8·10 |
| Eu | 1·27 | 1·56 | 1·90 | 2·51 | 3·19 |
| Tb | 0·55 | 0·71 | 0·65 | 0·97 | 0·88 |
| Yb | 1·27 | 1·62 | 1·18 | 1·59 | 1·81 |
| Lu | 0·18 | 0·21 | 0·14 | 0·22 | 0·26 |

*Table 1b: Compositional data for volcanic and plutonic rocks from Mount Ross in order of decreasing MgO (major elements in wt %; trace elements in ppm)*

| Sample: | 121 | 99 | 64.1 | 39 | 97 | 57 | 48 | 54 |
|---|---|---|---|---|---|---|---|---|
| Rock type: | G | BTA | G | BTA | BTA | BTA | BTA | BTA |
| $SiO_2$ | 46·55 | 48·68±0·02 | 49·22 | 49·53 | 50·52 | 49·60 | 51·19±0·06 | 51·87 |
| $TiO_2$ | 3·41 | 2·88±0·01 | 2·59 | 2·49 | 2·24 | 2·38 | 2·20±0·01 | 2·00 |
| $Al_2O_3$ | 17·27 | 17·36±0·04 | 16·79 | 17·12 | 18·51 | 19·05 | 18·04±0·05 | 19·47 |
| $Fe_2O_3$ | 11·82 | 11·33±0·01 | 11·71 | 11·04 | 9·42 | 9·34 | 9·58±0·01 | 8·64 |
| MnO | 0·16 | 0·17±0·01 | 0·19 | 0·20 | 0·17 | 0·15 | 0·17±0·01 | 0·16 |
| MgO | 5·32 | 3·98±0·05 | 3·85 | 3·51 | 3·19 | 2·95 | 2·86±0·07 | 2·40 |
| CaO | 8·43 | 7·16±0·91 | 6·28 | 6·73 | 7·13 | 7·81 | 6·47±0·01 | 7·36 |
| $Na_2O$ | 3·74 | 4·36±0·01 | 4·36 | 4·69 | 4·37 | 4·46 | 4·59±0·03 | 5·03 |
| $K_2O$ | 2·37 | 3·01±0·01 | 3·30 | 3·31 | 3·21 | 2·91 | 3·65±0·01 | 2·16 |
| $P_2O_5$ | 0·65 | 1·01±0·01 | 1·29 | 1·43 | 0·98 | 1·02 | 0·88±0·01 | 0·97 |
| Total | 99·71 | 99·94 | 99·59 | 100·05 | 99·72 | 99·67 | 99·63 | 100·05 |
| Rb | 43·0 | 62·3 | | 63·3 | 71·2 | 64·3 | 77·9 | 63·5 |
| Cs | | 0·29±0·03 | 0·48±0·06 | 0·31 | 0·57 | 0·57 | 0·36±0·07 | 0·49 |
| Sr | 945 | 965 | | 892 | 971 | 1056 | 864 | 993 |
| Ba | | 794 | | 939 | 921 | 831 | | 840 |
| Sc | 15·6 | 12·4±0·2 | 11·7±0·1 | 11·7 | 11·0 | 10·8 | 11·0±0·1 | 9·8 |
| V | | 112 | | 84 | 74 | 97 | | 71 |
| Cr | 45 | 9 | 12·0±0·6 | | 17 | 4 | 11·0±0·1 | 6 |
| Co | 40·7 | 27·8±0·3 | 25·8±0·1 | 20·8 | 21·3 | 22·5 | 18·6±0·1 | 17·1 |
| Ni | | 19 | | 12 | 25 | 17 | | 14 |
| Zn | | 101 | | 133 | 101 | 97 | | 97 |
| Ga | 22·0 | 21·3 | | 22·9 | 23·4 | 23·3 | 23·9 | 24·3 |
| Y | 22·9 | 28·7 | | 37·4 | 32·8 | 30·0 | 34·5 | 30·9 |
| Zr | | 363 | | 367 | 396 | 361 | | 384 |
| Nb | | 63 | | 73 | 71 | 62 | | 64 |
| Hf | 6·37 | 7·79±0·17 | 8·1±0·2 | 8·24 | 8·56 | 7·79 | 9·16±0·56 | 8·18 |
| Ta | 3·16 | 3·81±0·18 | 3·87±0·16 | 4·20 | 3·96 | 3·55 | 4·44±0·07 | 3·73 |
| Th | 5·36 | 6·53±0·28 | 7·02±0·05 | 6·9 | 8·1 | 7·2 | 8·10±0·77 | 7·6 |
| U | | 1·5 | 1·76 | 1·40 | 1·80 | 1·60 | 1·94 | 1·6 |
| Pb | | 5·1 | 5·7 | 5·4 | 5·7 | 4·8 | 6·3 | 5·2 |
| La | 43·1 | 56·8±0·2 | 67·2±2·2 | 67·7 | 64·7 | 57·5 | 70·4±2·8 | 61·7 |
| Ce | 94·1 | 124±0·1 | 144±1 | 154 | 143 | 126 | 154±1 | 136 |
| Nd | 40·4 | 54·6±1·3 | 63·4±0·1 | 69·1 | 60·8 | 54·8 | 64·8±0·1 | 57·9 |
| Sm | 7·98 | 10·4±0·1 | 11·8±0·4 | 14·0 | 11·6 | 10·9 | 11·8±0·3 | 10·8 |
| Eu | 2·64 | 3·38±0·07 | 3·88±0·05 | 4·32 | 3·48 | 3·41 | 3·58±0·03 | 3·68 |
| Tb | 0·86 | 1·14±0·05 | 1·30±0·12 | 1·56 | 1·30 | 1·13 | 1·30±0·05 | 1·11 |
| Yb | 2·22 | 2·34±0·09 | 2·53±0·10 | 2·73 | 2·67 | 2·30 | 2·75±0·30 | 2·63 |
| Lu | 0·27 | 0·31±0·01 | 0·35±0·02 | 0·37 | 0·33 | 0·32 | 0·39±0·01 | 0·35 |

syenite as the proportion of fluidal feldspar microlites decreases and the crystal size increases to coarse grained. The syenites contain sodic plagioclase, alkali feldspar, hedenbergite, Fe–Ti oxides, and late interstitial acmitic augite and nepheline; analcite and calcite are common secondary phases.

| Sample: | 130 | 142 | 38 | 144 | 107 | 61 | 44 | 98 |
|---|---|---|---|---|---|---|---|---|
| Rock type: | BTA | TA | TA | TA | TA | S | T | T |
| $SiO_2$ | 52·28 | 55·00 | 55·31 | 55·47 | 56·61 | 59·35 | 60·44 | 61·05 |
| $TiO_2$ | 1·82 | 1·57 | 1·31 | 1·27 | 1·09 | 0·64 | 0·49 | 0·49 |
| $Al_2O_3$ | 19·12 | 17·87 | 17·84 | 19·45 | 17·92 | 18·45 | 18·10 | 18·12 |
| $Fe_2O_3$ | 8·68 | 8·41 | 8·68 | 6·71 | 7·79 | 5·92 | 5·53 | 5·18 |
| MnO | 0·17 | 0·18 | 0·19 | 0·14 | 0·18 | 0·16 | 0·17 | 0·16 |
| MgO | 2·33 | 1·88 | 1·73 | 1·43 | 1·27 | 0·83 | 0·59 | 0·43 |
| CaO | 6·34 | 4·57 | 4·18 | 4·56 | 3·06 | 2·70 | 2·03 | 1·68 |
| $Na_2O$ | 4·56 | 5·03 | 5·13 | 5·17 | 5·70 | 5·45 | 6·24 | 6·18 |
| $K_2O$ | 3·52 | 4·58 | 4·63 | 4·37 | 5·61 | 5·78 | 5·91 | 6·35 |
| $P_2O_5$ | 0·86 | 0·60 | 0·62 | 0·59 | 0·43 | 0·26 | 0·15 | 0·11 |
| Total | 99·68 | 99·68 | 99·62 | 99·68 | 99·64 | 99·51 | 99·64 | 99·74 |
| Rb | 73·6 | 88·0 | | 114 | 142 | | 138·6 | 128 |
| Cs | 0·48 ± 0·01 | 0·38 | 0·42 ± 0·01 | 0·98 | 1·18 | 0·60 ± 0·01 | 1·19 | 0·93 |
| Sr | 949 | 736 | | 729 | 400 | | 115 | 26·1 |
| Ba | 971 | 2047 | | 1062 | 1153 | | 313 | 58 |
| Sc | 8·99 ± 0·01 | 11·9 | 9·5 ± 0·1 | 6·0 | 7·1 | 5·5 ± 0·1 | 6·7 | 5·7 |
| V | 47 | 19 | | 23 | 6 | | 5 | 1 |
| Cr | 7 ± 1 | | | 1·8 | 2 | 4 ± 1 | 2·5 | |
| Co | 13·7 ± 0·1 | 8·7 | 7·1 ± 0·1 | 8·4 | 5·7 | 4·3 ± 0·1 | 1·5 | 0·8 |
| Ni | 12 | 7 | | 17 | 16 | | 11 | 11 |
| Zn | 112 | 110 | | 89 | 131 | | 103 | 88 |
| Ga | 24·7 | 23·7 | | 25·7 | 26·4 | | 27·4 | 24·7 |
| Y | 33·3 | 34·9 | | 33·4 | 43·5 | | 43·4 | 37·0 |
| Zr | 442 | 475 | | 626 | 737 | | 796 | 641 |
| Nb | 78 | 84 | | 98 | 119 | | 126 | 101 |
| Hf | 8·84 ± 0·18 | 10·4 | 10·9 ± 4 | 12·8 | 16·3 | 14·9 ± 0·5 | 16·6 | 13·7 |
| Ta | 4·17 ± 0·06 | 4·71 | 4·80 ± 0·08 | 5·46 | 6·51 | 6·30 ± 0·13 | 6·83 | 5·63 |
| Th | 8·12 ± 0·13 | 9·29 | 9·1 ± 0·8 | 13·0 | 15·5 | 12·8 ± 0·6 | 15·2 | 12·5 |
| U | 1·90 | 1·70 | 2·05 | 3·00 | 3·30 | 3·04 | 3·50 | 2·70 |
| Pb | 6·1 | 7·4 | 8·1 | 8·6 | 10·2 | 10·4 | 11·7 | 10·7 |
| La | 67·5 ± 1·6 | 73·0 | 74·9 ± 2·4 | 77·6 | 91·8 | 90·2 ± 4 | 95·9 | 82·5 |
| Ce | 146 ± 2 | 154 | 158 ± 3 | 159 | 194 | 190 ± 9 | 196 | 170 |
| Nd | 61·4 ± 1·8 | 63·6 | 61·2 ± 0·6 | 61·1 | 74·5 | 72·3 ± 1 | 75 | 66·2 |
| Sm | 11·4 ± 0·5 | 11·6 | 11·0 ± 0·1 | 11·0 | 13·9 | 13·5 ± 0·7 | 12·7 | 11·6 |
| Eu | 3·66 ± 0·09 | 4·49 | 3·62 ± 0·02 | 3·23 | 3·72 | 2·23 ± 0·03 | 1·54 | 2·19 |
| Tb | 1·26 ± 0·09 | 1·32 | 1·22 ± 0·01 | 1·22 | 1·60 | 1·46 ± 0·02 | 1·63 | 1·44 |
| Yb | 2·60 ± 0·01 | 3·21 | 2·96 ± 0·20 | 2·84 | 4·12 | 3·68 ± 0·02 | 3·90 | 3·50 |
| Lu | 0·37 ± 0·01 | 0·42 | 0·40 ± 0·01 | 0·42 | 0·55 | 0·53 ± 0·02 | 0·57 | 0·54 |

## ANALYTICAL RESULTS

### K–Ar ages

Mount Ross volcano was built on an early Miocene basaltic basement containing intrusive gabbroic dikes which range in age from approximately 24 to 20 Ma (Table 2). Based on the K–Ar dates (Table 2) and field geology (Fig. 1), Mount Ross was probably constructed in several Pleistocene episodes. Volcanism began at ~1 Ma. The interval from 1 Ma to 0·4 Ma is represented by intrusive and extrusive rocks exposed at the head of the main eastern glacier (Buffon Glacier

*Table 1b: continued*

| Sample: | 131 | 29 | 106 | 108 | 143 | 112 |
|---|---|---|---|---|---|---|
| Rock type: | T | T | T | T | T | S |
| $SiO_2$ | 60·32 | 61·10 | 60·56 | 61·20 ± 0·09 | 61·00 ± 0·04 | 61·92 |
| $TiO_2$ | 0·41 | 0·39 | 0·27 | 0·24 ± 0·01 | 0·079 ± 0·001 | 0·125 |
| $Al_2O_3$ | 18·14 | 18·02 | 18·27 | 18·62 ± 0·06 | 18·87 ± 0·04 | 18·21 |
| $Fe_2O_3$ | 5·97 | 6·20 | 5·65 | 5·01 ± 0·01 | 4·87 ± 0·01 | 4·70 |
| MnO | 0·17 | 0·18 | 0·18 | 0·16 ± 0·01 | 0·17 ± 0·01 | 0·18 |
| MgO | 0·41 | 0·38 | 0·28 | 0·21 ± 0·04 | 0·16 ± 0·06 | 0·09 |
| CaO | 1·93 | 2·09 | 1·72 | 1·30 ± 0·01 | 1·19 ± 0·01 | 1·30 |
| $Na_2O$ | 6·06 | 6·28 | 6·82 | 6·76 ± 0·07 | 7·58 ± 0·06 | 7·32 |
| $K_2O$ | 6·07 | 5·92 | 5·92 | 6·08 ± 0·01 | 5·62 ± 0·02 | 5·52 |
| $P_2O_5$ | 0·13 | 0·13 | 0·07 | 0·051 ± 0·001 | 0·042 ± 0·002 | 0·037 |
| Total | 99·58 | 99·71 | 99·73 | 99·63 | 99·58 | 99·39 |
| Rb | 133 | 140·6 | 165 | 175 | 221 | |
| Cs | 0·93 | 1·11 | 1·22 | 1·33 ± 0·10 | 1·96 ± 0·07 | 2·07 |
| Sr | 150 | 190 | 3·8 | 16·5 | 7·7 | |
| Ba | 480 | 751 | | | | |
| Sc | 6·0 | 2·4 | 5·2 | 2·09 ± 0·01 | 0·17 ± 0·1 | 0·51 |
| V | | 0·90 | 0·06 | 3 | | |
| Cr | | | | | | |
| Co | 0·9 | 1·0 | 0·4 | 0·8 ± 0·1 | 0·25 ± 0·01 | 0·30 |
| Ni | 14 | 9 | 7 | 10 | 11 | |
| Zn | 117 | 113 | 113 | 119 | 186 | |
| Ga | 28·5 | 24·7 | 29·7 | 30·6 | 34·0 | |
| Y | 43·7 | 32·3 | 57·0 | 49·4 | 56·5 | |
| Zr | 806 | 787 | 1072 | 1347 | 1292 | |
| Nb | 118 | 115 | 184 | 174 | 181 | |
| Hf | 17·2 | 16·3 | 22·6 | 25·2 ± 1·3 | 27·8 ± 0·9 | 29·9 |
| Ta | 6·87 | 6·6 | 9·1 | 8·71 ± 0·13 | 11·8 ± 0·4 | 13·5 |
| Th | 14·5 | 14·9 | 17·6 | 20·0 ± 1·0 | 28·6 ± 0·6 | 34 |
| U | 3·20 | 3·40 | 3·70 | 3·30 | 6·40 | 7·20 |
| Pb | 10·8 | 5·4 | 12·6 | 13·8 | 19·9 | 19·6 |
| La | 98·3 | 90·0 | 122 | 122 ± 1 | 159 | 205 |
| Ce | 201 | 174 | 255 | 244 ± 2 | 311 ± 2 | 389 |
| Nd | 75·8 | 61·7 | 100 | 86 ± 2 | 97 ± 2 | 122 |
| Sm | 13·6 | 9·98 | 18·4 | 14·8 ± 0·4 | 16·1 ± 0·1 | 19·6 |
| Eu | 2·89 | 2·26 | 0·86 | 0·60 ± 0·01 | 0·66 ± 0·01 | 0·50 |
| Tb | 1·70 | 1·03 | 2·02 | 1·74 ± 0·08 | 1·82 ± 0·06 | 2·39 |
| Yb | 4·06 | 3·33 | 5·30 | 5·23 ± 0·20 | 5·27 | 7·49 |
| Lu | 0·59 | 0·44 | 0·76 | 0·76 ± 0·03 | 0·77 | 0·97 |

Rock types: G, gabbro; S, syenite; TB, trachybasalt; BTA, basaltic trachyandesites; TA, trachyandesite; T, trachyte; S, microsyenite. Uncertainties indicated for samples 99, 48, 130, 108 and 143 are deviations from the mean for analyses of two separate powders of the same rock. Uncertainties indicated for samples 64.1, 38 and 61 are deviations from the mean for duplicate neutron activation analyses of the same powder.

in Fig. 1). These samples range in texture from trachytic to syenitic and include an altered (unsampled) gabbro intrusion exposed at a low level in the central depression. Subsequently there were two intense eruptive periods. The first period, at ~0·25 Ma, is represented by gabbro and syenite exposed at the head of the Rouge Glacier

*Table 2: K–Ar ages of Mount Ross volcanic and plutonic rocks*

| Sample | Origin | Rock type | K (%) | Ar Atm. | % $^{40}$Ar (ng/g) | Age (Ma) | Error (Ma) |
|---|---|---|---|---|---|---|---|
| 91 | 1 | G | 1·99 | 48·6 | 3·57 | 24·3 | 0·5 |
| 83 | 1 | G | 0·743 | 44·5 | 1·12 | 21·7 | 0·4 |
| 78 | 1 | G | 0·993 | 42·8 | 1·45 | 21·0 | 0·4 |
| 145 | 1 | G | 0·641 | 49·4 | 0·890 | 19·9 | 0·4 |
| 143 | 4 | T | 4·65 | 84·3 | 0·329 | 1·02 | 0·06 |
| 112 | 2 | S | 4·56 | 88·2 | 0·202 | 0·64 | 0·05 |
| 108 | 2 | T | 4·91 | 95·9 | 0·128 | 0·38 | 0·09 |
| 61 | 3 | S | 4·73 | 91·0 | 0·0822 | 0·251 | 0·026 |
| 64.1 | 3 | G | 2·74 | 97·2 | 0·0446 | 0·235 | 0·083 |
| 130 | 4 | BTA | 3·05 | 91·1 | 0·044 | 0·21 | 0·02 |
| 48 | 4 | BTA | 2·98 | 89·5 | 0·0345 | 0·167 | 0·015 |
| 38 | 4 | TA | 3·91 | 89·3 | 0·0412 | 0·152 | 0·013 |
| 99 | 4 | BTA | 2·5 | 95·3 | 0·023 | 0·13 | 0·03 |

Origin: 1, basement; 2, head of the eastern glacier; 3, head of the western glacier; 4, flanks of the Ross volcano. Rock type as given in Table 1.

(samples 64.1 and 61 in Fig. 1b and Table 2). The last episode, from 0·20 to 0·13 Ma, is represented by the flanks of the present cone. Thus Mount Ross is a Pleistocene volcano constructed in <1 my and the youngest volcano discovered in the Kerguelen Archipelago.

## Major elements and compatible trace elements

In the total alkalis–$SiO_2$ plot (Fig. 2a) commonly used for classification of volcanic rocks (Le Bas *et al.*, 1986), the Mount Ross lavas lie within the alkalic field with rock types varying from basaltic trachyandesite to trachyte. They have high $K_2O/Na_2O$ ratios, typically ~0·7–1 (Table 1b). The oldest lavas associated with the Kerguelen plume are tholeiitic basalt, e.g. the Kerguelen Plateau (Storey *et al.*, 1992; Mahoney *et al.*, 1995) and Ninetyeast Ridge (Frey *et al.*, 1991). Previous studies of Kerguelen Archipelago lavas suggested that lava compositions became increasingly alkalic with decreasing age (e.g. Storey *et al.*, 1988; Gautier *et al.*, 1990; Weis *et al.*, 1993). However, Mount Ross samples, the youngest lavas erupted in the Kerguelen Archipelago, define a trend that is intermediate in alkalinity to the Upper and Lower Miocene lavas from the Southeast Province (Fig. 2b). Therefore, the Mount Ross data show a reversal of the trend for increasing alkalinity with decreasing age. The basement rocks for Mount Ross include three 19·9–21·7 Ma gabbros with <5% total alkalis, a 24·3 Ma gabbro (sample 91) with a basaltic trachyandesite composition and a trachybasalt (Tables 1a and 2; Fig. 2a).

Lavas from Mount Ross form well-defined trends in MgO variation plots and the four plutonic rocks from Mount Ross lie on these trends (Fig. 3). Importantly, the Lower Miocene alkali basalts and trachytes lie on extensions of the Mount Ross trends. When grouped together the Mount Ross and Lower Miocene lavas define inflected trends for abundances of $Fe_2O_3$ (total iron), $TiO_2$, $P_2O_5$, V and Sc vs MgO content (Fig. 3). The basement rocks from the vicinity of Mount Ross, however, deviate from these trends to lower $Fe_2O_3$ and $TiO_2$ (Fig. 3). Among the 22 Mount Ross samples, the highest MgO content (5·32%) is in a young gabbro (sample 121) that has relatively high iron and titanium; another gabbro (sample 64.1) has one of the highest $P_2O_5$ contents (Fig. 3). Both gabbros contain olivine, clinopyroxene, Fe–Ti oxides and apatite. The MgO variation trends for these basalt to trachyte suites indicate an important role for fractionation of clinopyroxene, Fe–Ti oxides and apatite. Specifically, the positive CaO–MgO trend and marked increase in $Al_2O_3/CaO$ with decreasing MgO reflect clinopyroxene segregation. The inflected trends of MgO–$TiO_2$ and MgO–$P_2O_5$ reflect the onset of Fe–Ti oxide and apatite segregation, respectively. The important role of these phases is also indicated by the positive trends of V (Fe–Ti oxide control) and Sc (clinopyroxene control) with MgO content (Fig. 3). Magmas with ~6% MgO were saturated in clinopyroxene whereas significant fractionation of Fe–Ti oxides and

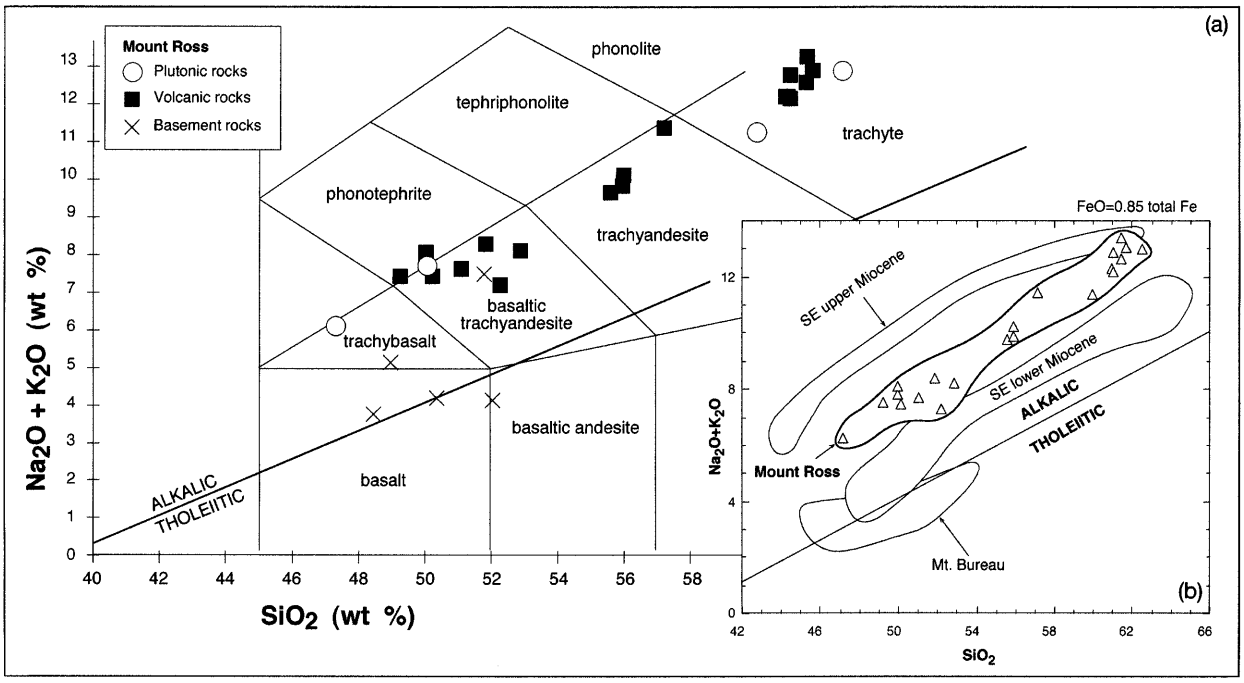


**Fig. 2.** Total alkalis vs $SiO_2$ (all in wt % with FeO = 0·85 of total iron content). In (a) the Mt Ross and basement rocks are plotted in the classification diagram of Le Bas *et al.* (1986). (b) shows archipelago lavas relative to the Hawaiian boundary between tholeiitic and alkaline lavas (MacDonald & Katsura, 1964). Mt Ross lavas are more alkalic than the flood basalts at Mount Bureau on Foch Island (Yang *et al.*, 1998) and they are intermediate between the Upper and Lower Miocene groups in the Southeast Province (Weis *et al.*, 1993).

apatite commenced at ~5·3% and 3·8% MgO, respectively (Fig. 3).

## Incompatible elements

The elements Cs, Rb, U, Th, La, Ce, Pb, Nb, Ta, Zr and Hf were incompatible during the petrogenesis of Mount Ross lavas (Fig. 4). The strongly positive correlations between abundances of the mobile elements Cs, Rb and U with less mobile elements such as Th, Ta and Hf (Fig. 4) indicate that the whole-rock compositions were not significantly modified by post-magmatic alteration. The largest abundance ranges are for Th (factor of 6·3) and Cs (factor of 7·1). As for major element abundances (Fig. 3), plutonic and volcanic rocks from Mount Ross lie on the same incompatible element trends (Fig. 4); there is no evidence that the gabbros and syenites are cumulate rocks. The incompatible element correlations determined by the basalt to trachyte sequences of different age, i.e. Lower Miocene series from the Southeast Province and the <1 Ma Mount Ross rocks, are very similar (Fig. 4).

Assuming that the compositional variation among Mount Ross lavas was largely controlled by fractional crystallization and that the bulk solid–melt partition coefficients for Th and Cs were approximately zero, the Th and Cs abundance ranges in Mount Ross rocks require that the most evolved syenite (sample 112) represents a residual melt formed after 85% crystallization of the most mafic magma (gabbro 121). It is not our purpose here to quantitatively evaluate the relationship between the Mount Ross trachytes–syenites and the associated more mafic lavas; this is better done for volcanoes which are more amenable to detailed sampling and field study. Nevertheless, like the major and compatible trace elements, the abundance trends of incompatible trace elements in Mount Ross lavas are consistent with control by mineral–melt fractionation. The trace elements Sr, Eu and Ba, which are normally incompatible during the petrogenesis of basaltic magmas, were compatible during the evolution of Mt Ross lavas; for example, the abundance ratio Sr/Nd, which is a sensitive indicator of feldspar fractionation, decreases with increasing Th content (Fig. 5). The four most evolved Mount Ross rocks (0·09–0·28% MgO), have very significant depletions in Eu (Fig. 6). Also, the trachytes have especially low Ba/Rb ratios, <5·3 (Fig. 7), which reflects the compatibility of Ba in alkali-rich feldspar (Blundy & Wood, 1991). Therefore, the abundance trends for Sr, Eu and Ba

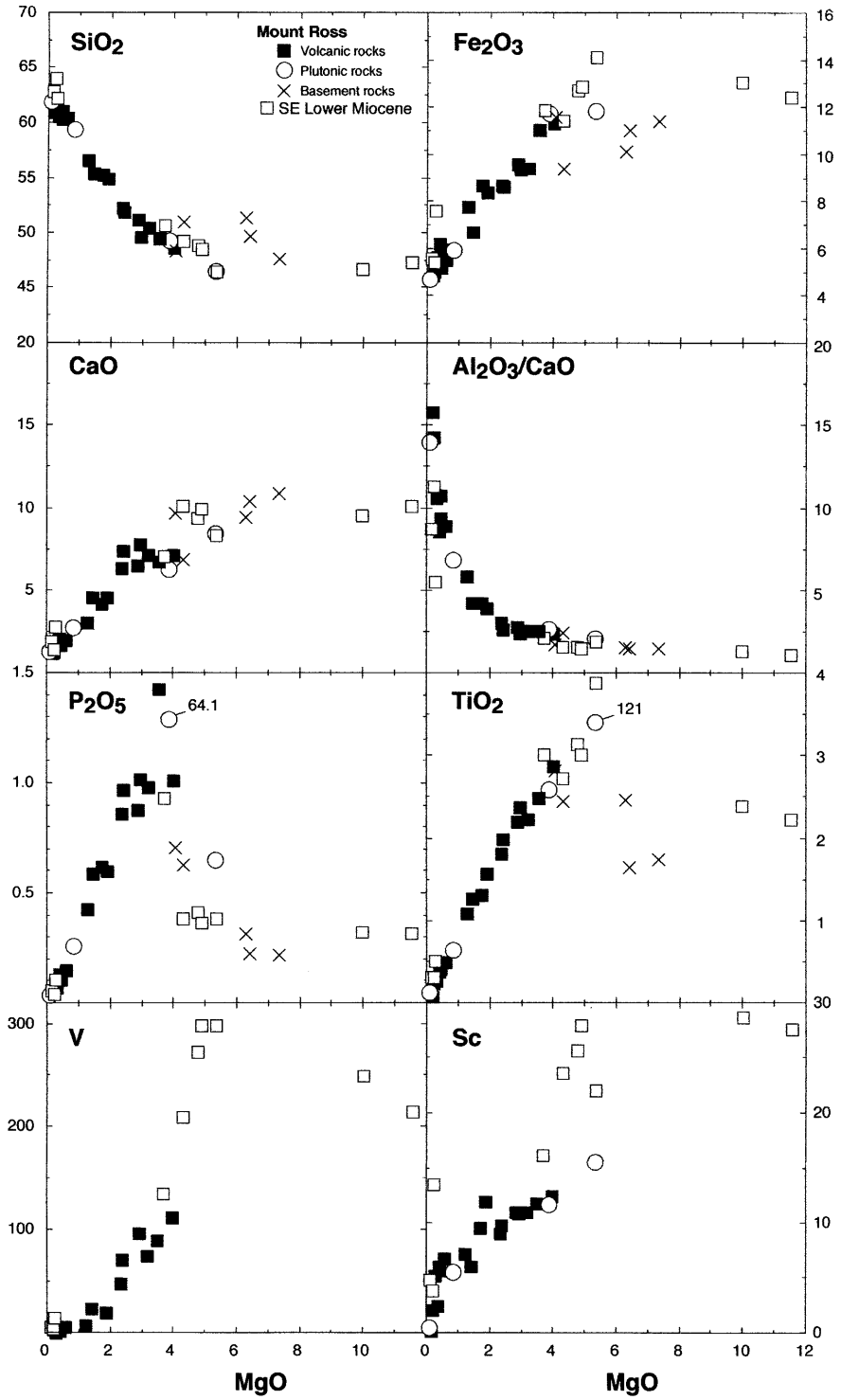


**Fig. 3.** Abundances of major oxides (wt %), Sc and V (ppm) and $Al_2O_3/CaO$ vs MgO content (wt %) in volcanic and plutonic rocks from Mount Ross and the surrounding >20 Ma basement (Table 1). The mean of 22 analyses of Mount Ross trachytes determined by Nougier (1970) is similar to the new data. The observed trends reflect the role of clinopyroxene, Fe–Ti oxides and apatite fractionation. Data are also shown for the Lower Miocene alkalic basalt to trachyte series from the Southeast Province (Weis *et al.*, 1993) which ranges to higher MgO contents than the Mount Ross lavas. The trends are very similar for these lavas series of very different age.

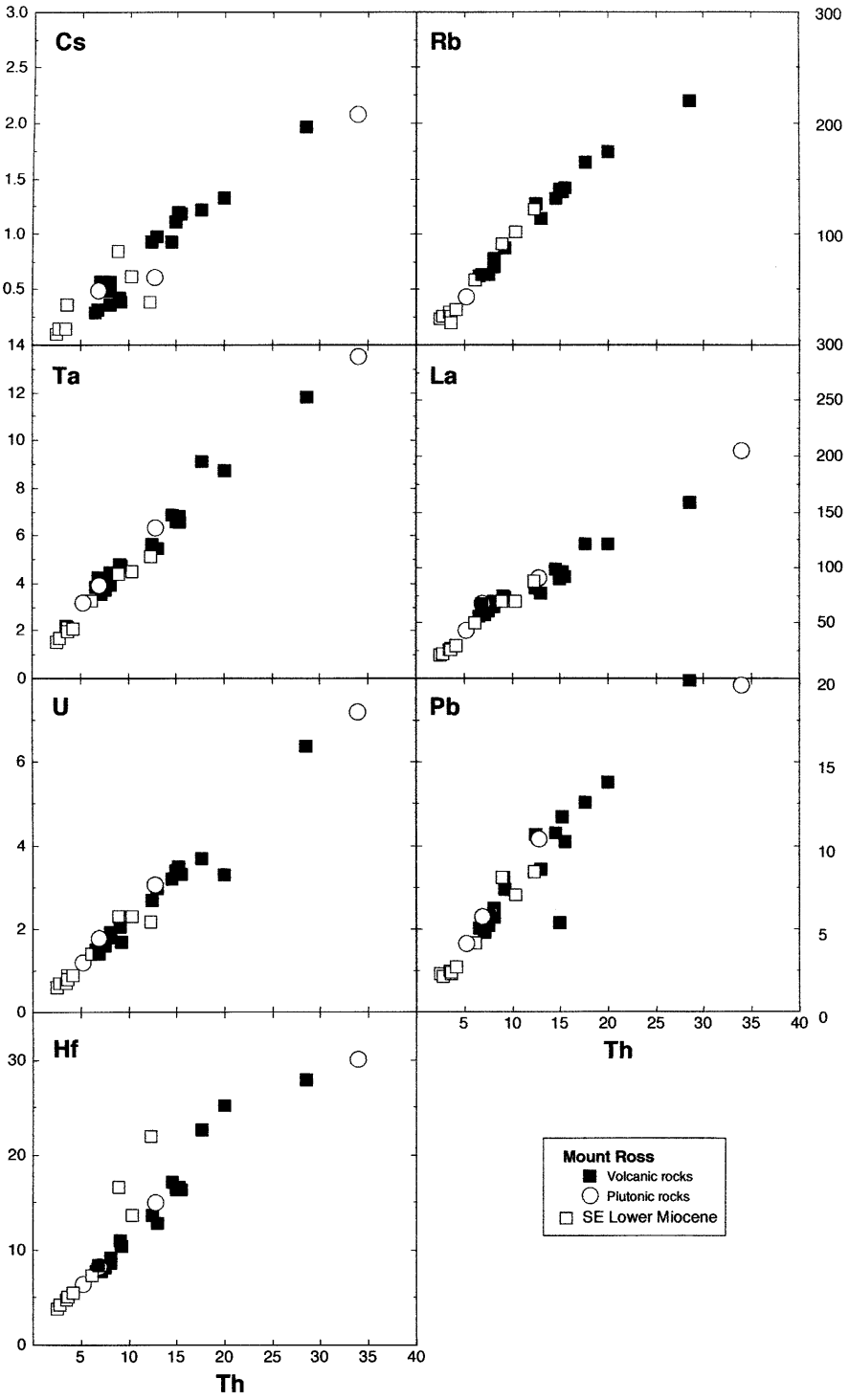


**Fig. 4.** Abundance of various incompatible elements vs Th content (all in ppm) for plutonic and volcanic rocks from Mt Ross (Table 1b). We use Th as a fractionation index because it is immobile, has a large range in abundance and Th was determined in all samples. These abundances are strongly correlated in both the volcanic and plutonic rocks. With few exceptions the Lower Miocene and Mount Ross alkali basalt to trachyte lavas lie on the same trend.

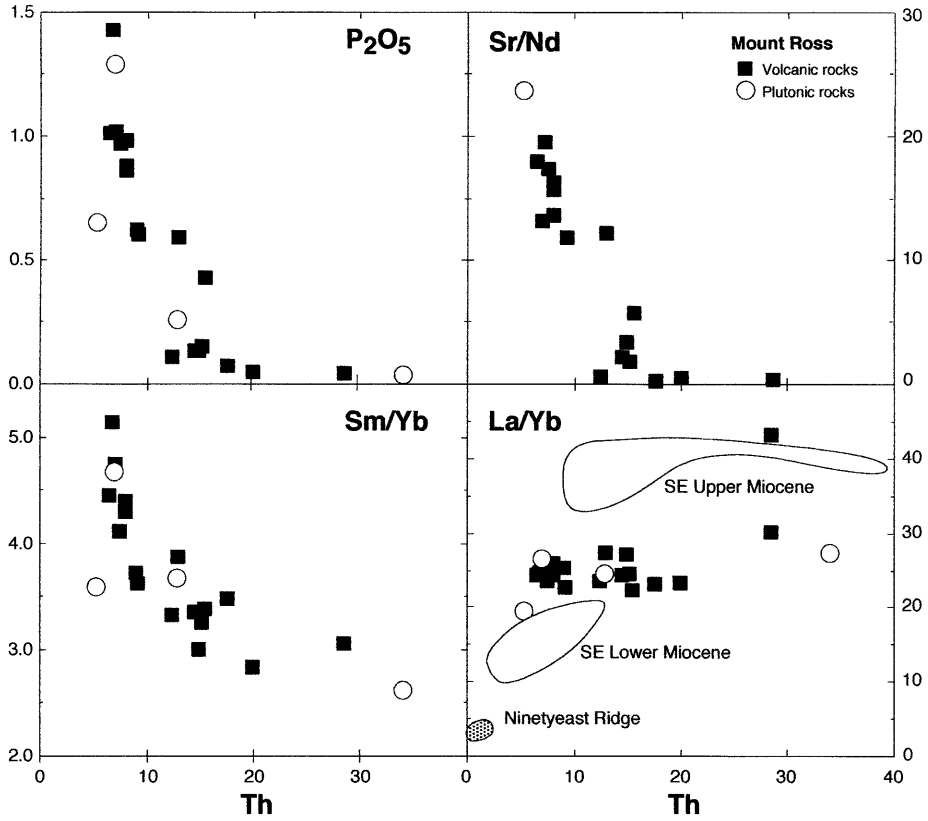


**Fig. 5.** Abundance of $P_2O_5$ (wt %) and the abundance ratios Sr/Nd, Sm/Yb and La/Yb vs Th content (ppm) for Mt Ross rocks. The negative slopes reflect segregation of apatite ($P_2O_5$ and Sm/Yb trends) and feldspar (Sr/Nd trend). Shown for comparison in the La/Yb panel are fields for the Lower Miocene and Upper Miocene series of the SE Province (Weis *et al.*, 1993) and basalts from the Ninetyeast Ridge (Frey *et al.*, 1991). The increasing Th and La/Yb from the Ninetyeast Ridge to Lower Miocene to Mount Ross is consistent with a temporal decrease in the extent of melting.

unambiguously demonstrate the importance of feldspar segregation during the petrogenesis of Mount Ross trachytes and syenites.

An important role for apatite segregation during evolution of the Mount Ross magmas is indicated by the positive $P_2O_5$–MgO trends (Fig. 3) and negative $P_2O_5$–Th trend (Fig. 5). Apatite segregation also significantly affected REE abundances. Normally both La/Yb and Sm/Yb increase with increasing differentiation of basaltic magmas. Apatite, however, preferentially incorporates intermediate atomic number REE, such as Sm, relative to light REE and heavy REE (Watson & Green, 1981). Consequently, Mount Ross lavas and plutonic rocks define a trend of decreasing Sm/Yb with increasing Th content (Fig. 5). The decrease in Sm/Yb, approximately a factor of two (Fig. 5), can be explained by 1·5% apatite in the segregating cumulate (assuming 85% total crystallization and apatite–liquid partition coefficients ($D$) of 40 and 20 for Sm and Yb, respectively). Apatite segregation may also explain the decrease in Ce/Pb with increasing Th content (Fig. 7).

The systematic increases in Zr/Nb and Th/Ta and decrease in Nb/U with increasing Th content (Fig. 7) can be explained by ~8% titanomagnetite in the crystallizing assemblage [assuming titanomagnetite $D$ values of 0, 2·16 and 0·24, for Th–U, Ta–Nb and Zr, respectively (Spath *et al.*, 1996)]. The precipitous decrease in V content with decreasing MgO content (Fig. 3) can also be explained by ~8% titanomagnetite in the fractionating assemblage [assuming $D = 20$ for V in titanomagnetite (Spath *et al.*, 1996)]; this amount of titanomagnetite in the segregating assemblage is consistent with inferences from studies of other volcanic suites (e.g. le Roex, 1985).

Although the processes that created the trachytes significantly changed many incompatible element abundance ratios, these ratios in the most mafic Mount Ross lavas (i.e. <10 ppm Th) are typical for ocean island basalts (Fig. 7). However, compared with the tholeiitic

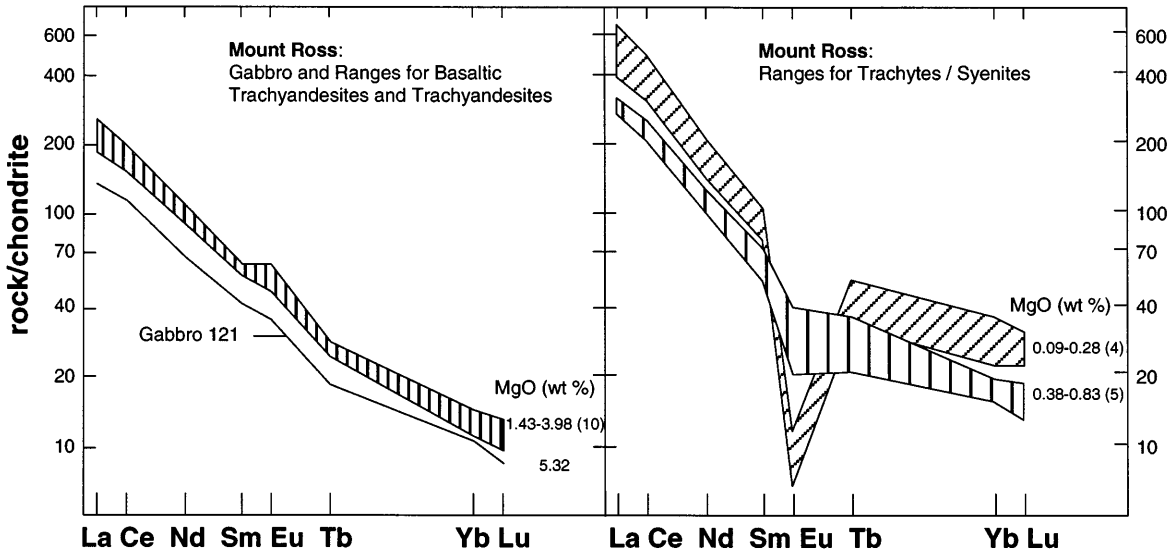


**Fig. 6.** Chondrite-normalized [recommended average of Boynton (1984)] REE patterns for Mount Ross rocks grouped on the basis of MgO content. The number within parentheses indicates the number of samples that define the ranges.

basalts which form the Ninetyeast Ridge (Frey *et al.*, 1991) and Kerguelen Plateau (Storey *et al.*, 1992), the most mafic Mount Ross lavas and the Miocene alkali basalts and basanites of the Southeast Province are highly enriched in incompatible elements such as Th; they also have higher La/Yb (Fig. 5).

## Sr, Nd and Pb isotopic ratios

The flood basalts forming the archipelago range widely in radiogenic isotopic ratios (Table 3), even in a single stratigraphic section (Yang *et al.*, 1998). Flood basalts with the highest $^{87}Sr/^{86}Sr$ and lowest $^{143}Nd/^{144}Nd$ and $^{206}Pb/^{204}Pb$, such as the lowermost, ~30 Ma, lavas on Foch Island in the northern part of the archipelago (Fig. 1a), overlap with the isotopic ratios of the Upper Miocene lavas erupted in the Southeast Province of the archipelago (Fig. 8a). Weis *et al.* (1993) proposed that these Upper Miocene lavas are the purest representation of the Kerguelen plume. The nine most mafic Mount Ross lavas and gabbros (2·3–5·3% MgO) have similar Sr, Nd and Pb isotopic ratios which overlap with the Upper Miocene field in Pb–Pb isotopic ratios (Fig. 8b) and form an $^{87}Sr/^{86}Sr$–$^{143}Nd/^{144}Nd$ field that is intermediate to the fields for Upper and Lower Miocene lavas from the Southeast Province (Fig. 8a). In an $^{87}Sr/^{86}Sr$–$^{206}Pb/^{204}Pb$ plot, these nine relatively mafic Mount Ross samples cluster below the Upper Miocene field at slightly lower $^{87}Sr/^{86}Sr$; that is, they have the low $^{206}Pb/^{204}Pb$ ratios, <18·2, that are characteristic of the Upper Miocene lavas (Fig. 8c).

Using measured or inferred ages and measured Rb/Sr, we find that the initial $^{87}Sr/^{86}Sr$ for eight of ten trachyandesites and trachytes (Rb and Sr contents are not available for the two syenites and trachyandesite 38) are within 3 SD (0·00015) of the mean of the nine more mafic rocks (0·70519 $\pm$ 5; Table 3 and see expanded panels in Fig. 8a and c). For trachyte 106, which has a slightly higher initial $^{87}Sr/^{86}Sr$, we have only an inferred age (Table 3); if this sample is slightly older, its initial ratio overlaps with that of the mafic rocks. However, trachyte 108 is isotopically distinct. Its age, 0·38 $\pm$ 0·09 Ma, is not very precise, but an initial $^{87}Sr/^{86}Sr$ ratio similar to the more mafic samples requires a much older age of 2·8 Ma; this sample also has relatively low $^{206}Pb/^{204}Pb$. The measured $^{143}Nd/^{144}Nd$ in all of the trachyandesites, trachytes and syenites are within 2 SD (0·00010) of the mean for the nine more mafic rocks (0·51258 $\pm$ 1); only trachyandesite 38 is slightly offset from the field for relatively mafic Mount Ross rocks to higher $^{143}Nd/^{144}Nd$ (Fig. 8a). Similarly for $^{206}Pb/^{204}Pb$, 11 of the 13 trachyandesites, trachytes and syenites are within 2 SD (0·036) of the mean for the nine more mafic rocks (18·106 $\pm$ 18). Despite the two outliers and the difficulty with age corrections for $^{87}Sr/^{86}Sr$, the important result is that all of the Mount Ross samples, including volcanic and plutonic rocks, have the combination of relatively high $^{87}Sr/^{86}Sr$ and low $^{206}Pb/^{204}Pb$ that is characteristic of the Upper Miocene lavas from the Southeast

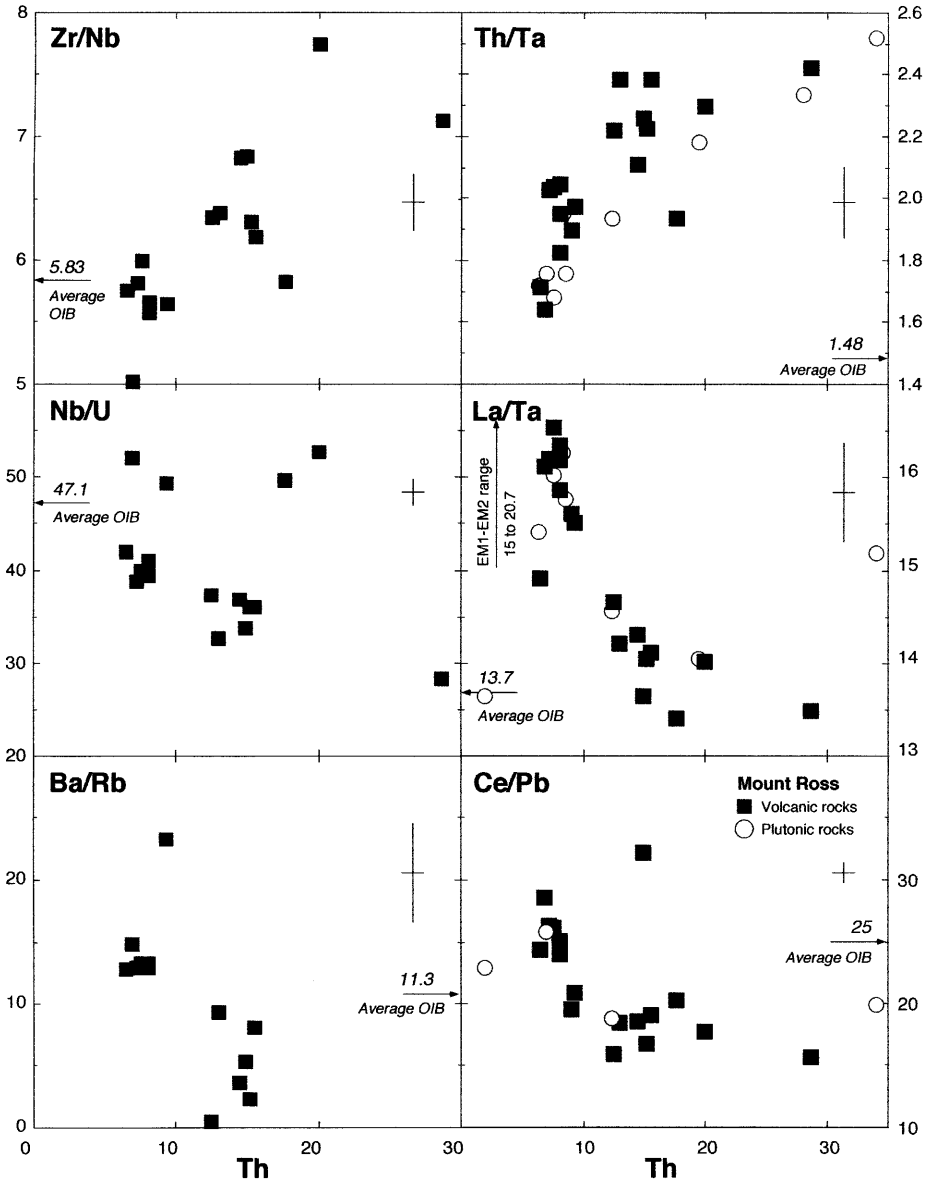


**Fig. 7.** Abundance ratios vs Th content (ppm) in Mount Ross lavas. These ratios are usually constant in basaltic suites but in Mount Ross rocks they vary as a result of extensive fractionation of feldspar, apatite and Fe–Ti oxides. It should be noted that the increase in Zr/Nb with increasing differentiation is opposite to the trend caused by fractionation of olivine, pyroxenes and plagioclase; this reversal reflects the segregation of Fe–Ti oxides. Error bars indicate 2 SD. Arrows with numbers on vertical axes indicate average OIB values from Sun & McDonough (1989), with the range for La/Ta in EM1 and EM2 lavas from Weaver (1991).

Province (Fig. 8) and that has been interpreted to be characteristic of the Kerguelen plume (Weis *et al.*, 1993).

In contrast to Mount Ross samples, the five basement samples, >20 Ma (Table 2), range to lower $^{87}Sr/^{86}Sr$ and higher $^{143}Nd/^{144}Nd$ (Fig. 8a); four of these samples have higher $^{206}Pb/^{204}Pb$ than any of the Mount Ross samples (Fig. 8b). Consequently, these basement samples are isotopically distinct from younger archipelago lavas, but their ratios are within the range of other archipelago flood basalts of comparable age (Fig. 8). The anomalously high $^{143}Nd/^{144}Nd$ of trachyandesite 38 may reflect contamination by similar basement rocks but the offset of some evolved lavas to lower $^{206}Pb/^{204}Pb$ (samples 108 and 143), lower $^{143}Nd/^{144}Nd$ (sample 143) or higher $^{87}Sr/^{86}Sr$ (sample 108) cannot be explained by a component from these basement rocks.

*Table 3: Sr, Nd and Pb isotopic data and Pb and U concentrations by isotope dilution for basement rocks and for volcanic and plutonic rocks from Mount Ross in order of decreasing MgO*

| Sample | Rock type* | $^{87}Rb/^{86}Sr$ | $^{87}Sr/^{86}Sr$ | $2\sigma_m$ | $^{87}Sr/^{86}Sr$ init | $^{143}Nd/^{144}Nd$ | $2\sigma_m$ | U† (ppm) | Pb† (ppm) | $^{238}U/^{204}Pb$ | $^{206}Pb/^{204}Pb$ | $^{207}Pb/^{204}Pb$ | $^{208}Pb/^{204}Pb$ |
|---|---|---|---|---|---|---|---|---|---|---|---|---|---|
| *Basement rocks* | | | | | | | | | | | | | |
| 145 | G | na | 0·704808 | 6 | | 0·512673 | 7 | 0·37 | 1·6 | 14·9 | 18·346 | 15·444 | 38·84 |
| | | | 0·704844 | 8 | | | | | | | | | |
| 83 | G | na | 0·705023 | 7 | | 0·512658 | 7 | 0·48 | 1·4 | 21·3 | 18·017 | 15·488 | 38·39 |
| | | | 0·705036 | 7 | | | | | | | | | |
| 78 | G | na | 0·705486 | 6 | | 0·512590 | 9 | 0·46 | 1·9 | 15·2 | 18·397 | 15·557 | 39·01 |
| 91 | G | na | 0·705120 | 7 | | 0·512622 | 7 | 1·20 | 5·4 | 14·2 | 18·327 | 15·546 | 38·90 |
| 128 | TB | na | 0·704999 | 7 | | 0·512614 | 12 | 0·84 | 2·8 | 19·2 | 18·380 | 15·547 | 38·96 |
| *Volcanic and plutonic rocks* | | | | | | | | | | | | | |
| 121 | G | 0·132 | 0·705167 | 7 | 0·70517‡ | 0·512601 | 7 | 1·20 | 4·1 | 18·5 | 18·080 | 15·530 | 38·51 |
| 99 | BTA | 0·187 | 0·705267 | 6 | 0·70527‡ | 0·512586 | 8 | 1·50 | 5·1 | 18·6 | 18·100 | 15·548 | 38·57 |
| 64 | G | na | 0·075243 | 6 | | 0·512573 | 7 | 1·76 | 5·7 | 19·5 | 18·097 | 15·552 | 38·57 |
| 39 | BTA | 0·205 | 0·075125 | 8 | 0·70512 | 0·512582 | 8 | 1·40 | 5·4 | 16·4 | 18·139 | 15·553 | 38·58 |
| 97 | BTA | 0·212 | 0·075215 | 6 | 0·70521 | 0·512565 | 8 | 1·80 | 5·7 | 20·1 | 18·099 | 15·553 | 38·58 |
| 57 | BTA | 0·176 | 0·075156 | 7 | 0·70516 | 0·512567 | 8 | 1·60 | 4·8 | 21·1 | 18·102 | 15·544 | 38·54 |
| 48 | BTA | 0·261 | 0·075233 | 6 | 0·70523‡ | 0·512586 | 8 | 1·94 | 6·3 | 19·5 | 18·093 | 15·554 | 38·58 |
| 54 | BTA | 0·185 | 0·075172 | 7 | 0·70517 | 0·512576 | 8 | 1·60 | 5·2 | 19·5 | 18·119 | 15·550 | 38·58 |
| | | | 0·075235 | 6 | | | | | | | | | |
| 130 | BTA | 0·224 | 0·075201 | 7 | 0·70520‡ | 0·512574 | 8 | 1·90 | 6·1 | 19·7 | 18·125 | 15·554 | 38·60 |
| | | | 0·075216 | 6 | | | | | | | | | |
| 142 | TA | 0·346 | 0·075208 | 8 | 0·70521 | 0·512564 | 8 | 1·70 | 7·4 | 14·5 | 18·199 | 15·548 | 38·58 |
| 38 | TA | na | 0·075234 | 7 | | 0·512626 | 14 | 2·05 | 8·1 | 16·0 | 18·112 | 15·558 | 38·60 |
| | | | 0·075269 | 6 | | | | | | | | | |
| 144 | TA | 0·453 | 0·075134 | 17 | 0·70513 | 0·512567 | 13 | 3·00 | 8·6 | 22·1 | 18·116 | 15·547 | 38·60 |
| 107 | TA | 1·03 | 0·075179 | 8 | 0·70518 | 0·512587 | 7 | 3·30 | 10·2 | 20·5 | 18·115 | 15·553 | 38·60 |
| 61 | S | na | 0·075249 | 7 | | 0·512571 | 9 | 3·04 | 10·4 | 18·5 | 18·101 | 15·547 | 38·57 |
| 44 | T | 3·49 | 0·075344 | 6 | 0·70533 | 0·512550 | 15 | 3·50 | 11·7 | 18·9 | 18·109 | 15·555 | 38·61 |
| 98 | T | 14·2 | 0·075482 | 6 | 0·70544 | 0·512555 | 7 | 2·70 | 10·7 | 16·0 | 18·100 | 15·561 | 38·64 |
| 131 | T | 2·57 | 0·075378 | 6 | 0·70537 | 0·512562 | 7 | 3·20 | 10·8 | 18·8 | 18·077 | 15·551 | 38·60 |
| 29 | T | 2·14 | 0·075198 | 6 | 0·70519 | 0·512580 | 8 | 3·40 | 5·4 | 38·8 | 18·097 | 15·545 | 38·55 |
| 106 | T | 126 | 0·075990 | 9 | 0·70563 | 0·512546 | 9 | 3·70 | 12·6 | 18·6 | 18·099 | 15·549 | 38·61 |
| 108 | T | 30·7 | 0·076493 | 8 | 0·70633‡ | 0·512542 | 8 | 3·30 | 13·8 | 15·1 | 18·025 | 15·547 | 38·56 |
| | | | 0·076419 | 6 | 0·70625‡ | 0·512515 | 7 | 3·20 | | | | | |
| 143 | T | 83·1 | 0·076525 | 8 | 0·70532‡ | 0·512503 | 8 | 6·40 | 19·9 | 20·3 | 18·026 | 15·542 | 38·58 |
| 112 | S | na | 0·076788 | 8 | | 0·512535 | 7 | 7·20 | 19·6 | 23·2 | 18·047 | 15·545 | 38·60 |

*Rock type as given in Table 1. na, not available. †Isotope dilution data. ‡Correction for *in situ* $^{87}Rb$ decay for K–Ar age as given in Table 2. Otherwise correction for 0·2 Ma. Parent–daughter abundance ratios are calculated from data in Table 1. The $2\sigma$ uncertainties for $^{87}Sr/^{86}Sr$ and $^{143}Nd/^{144}Nd$ indicate variation in last significant digits.

## DISCUSSION

### Magma supply rate

From ~115 to 38 Ma, i.e. during growth of the Kerguelen Plateau and Ninetyeast Ridge (Fig. 1a), tholeiitic basalt was the dominant magma type derived from the Kerguelen plume (Weis *et al.*, 1992). However, the flood basalts forming the Kerguelen Archipelago range from transitional basalt to alkalic lavas, with alkalic lavas becoming dominant with decreasing eruption age (Watkins *et al.*, 1974; Storey *et al.*, 1988; Gautier *et al.*, 1990; Weis *et al.*, 1993; Nicolaysen *et al.*, 1996; Yang *et al.*, 1998). Also, the magma supply rate has decreased from a relatively high rate, >1·5 $km^3$/yr, during growth of the Kerguelen Plateau to a much lower rate during the ~40 my growth of the Kerguelen Archipelago (Saunders *et al.*, 1994). These systematic long-term changes in magma composition and supply rate may represent the evolutionary stages of plume-derived volcanism; i.e. initial high volume magmatism derived from a plume-head (Kerguelen Plateau) followed by long-term magmatism derived from the plume-tail (Ninetyeast Ridge) followed by a gradual decrease in plume-derived volcanism as the supply of plume material is strongly reduced (Kerguelen Archipelago).

Magma supply rates during growth of the archipelago are ~0·013 $km^3$/yr [calculated for 8500 $km^2$ area, a crustal depth of 20 km (Recq *et al.*, 1990) and an eruption period from 40 to 24 Ma for the flood basalts (Nicolaysen *et al.*, 1996)]. This rate is much lower than that for Hawaiian shields (0·1 $km^3$/yr, Swanson, 1972), although it would be significantly increased, by a factor of 50 (to 0·5 $km^3$/yr), if the submarine part of the Northern Kerguelen Plateau is also <40 Ma (Coffin & Eldholm, 1994). This much higher rate is similar to that estimated during the formation of the Ninetyeast Ridge from ~82 to 38 Ma (Saunders *et al.*, 1994). It is obviously important to determine the basement age of the unsampled submarine portion of the northern Kerguelen Plateau. The alkalic magmatism and diminished magma supply rate represented by the archipelago may also reflect a changing tectonic environment (Storey *et al.*, 1988; Gautier *et al.*, 1990; Saunders *et al.*, 1994). Specifically, if the archipelago formed on the thick Cretaceous lithosphere of the Kerguelen Plateau, the effects of thickened lithosphere on plume-derived magmatism are to lower the extents of melting and increase the mean pressures of melt segregation (e.g. Ellam, 1992). The result is transitional to alkalic parental magmas showing the effects of residual garnet during partial melting, as indicated by La/Yb >10 in archipelago lavas compared with <4 in Ninetyeast Ridge tholeiites (Fig. 5 and Weis *et al.*, 1992; Saunders *et al.*, 1994; Frey & Weis, 1995).

Throughout the Miocene to recent growth of the archipelago, the abundance of evolved rocks, trachytes and phonolites in the Southeast Province (Weis *et al.*, 1993), and granites and syenites in the Rallier du Baty peninsula (Dosso *et al.*, 1979; Weis & Giret, 1994), show that the supply rate of basaltic magma to the crust decreased greatly after formation of the >20 Ma flood basalts which form ~85% of the surface outcrop (Fig. 1). At Mount Ross the absence of high-MgO lavas and the abundant trachytes show that the supply of basaltic parental magma remained low during the youngest phase of volcanism in the archipelago, that is, there was sufficient time for cooling of parental magmas and formation of evolved lavas by extensive mineral segregation. The similarity of the alkali basalt to trachyte suites erupted in the Lower Miocene, 20–22 Ma, in the Southeast Province and at Mount Ross, <1 Ma (Figs 3, 4, and 8), shows that petrogenetic processes have been similar for 22 my. Based on differences in incompatible element abundances of the most mafic lavas, the most significant geochemical trend over the past 22 my has been varying extents of melting; relatively high in the Lower Miocene (20–22 Ma), low in the Upper Miocene (6–10 Ma) and intermediate for the <1 Ma Mount Ross lavas (Fig. 2b and La/Yb panel in Fig. 5).

### Lithosphere assimilation: the role of the Cretaceous Kerguelen Plateau

There were three episodes of volcanism in the southeast part of the archipelago; the Pleistocene basaltic trachyandesite to trachyte lavas at Mount Ross, the Upper Miocene basanite to phonolite lavas in the Southeast Province and the Lower Miocene alkalic basalt to trachyte lavas in the Southeast Province. These spatially and temporally associated mafic and highly evolved lavas can be used to evaluate the role of shallow lithospheric

**Fig. 8.** (a) $^{87}Sr/^{86}Sr$ vs $^{143}Nd/^{144}Nd$, (b) $^{207}Pb/^{204}Pb$ vs $^{206}Pb/^{204}Pb$ and (c) $^{87}Sr/^{86}Sr$ vs $^{206}Pb/^{204}Pb$. $^{87}Sr/^{86}Sr$ data for Mount Ross samples are initial ratios using measured or inferred ages and Rb/Sr abundance ratios (Table 3); however, Rb/Sr data are not available for a few samples, such as syenite 112 whose offset to very high $^{87}Sr/^{86}Sr$ reflects the lack of an age correction. Field for Kerguelen Archipelago flood basalts is from Yang *et al.* (1998) and Damasceno *et al.* (1997). Most (85%) of the flood basalts from Mount Bureau and Mount Rabouillère have $^{87}Sr/^{86}Sr$ >0·7050, $^{143}Nd/^{144}Nd$ <0·5127 and $^{206}Pb/^{204}Pb$ <18·3, and they define isotopic fields which overlap with that of the most mafic Mount Ross lavas. Fields for Lower and Upper Miocene Series of the Southeast Province in the Kerguelen Archipelago are from Weis *et al.* (1993); trend for Heard Island defined by diamonds is from Barling *et al.* (1994). Expanded panels in $^{87}Sr/^{86}Sr$ vs $^{143}Nd/^{144}Nd$ and $^{87}Sr/^{86}Sr$ vs $^{206}Pb/^{204}Pb$ plots show the isotopic similarity of most trachytes, trachyandesites and syenites with the more mafic lavas and gabbros.

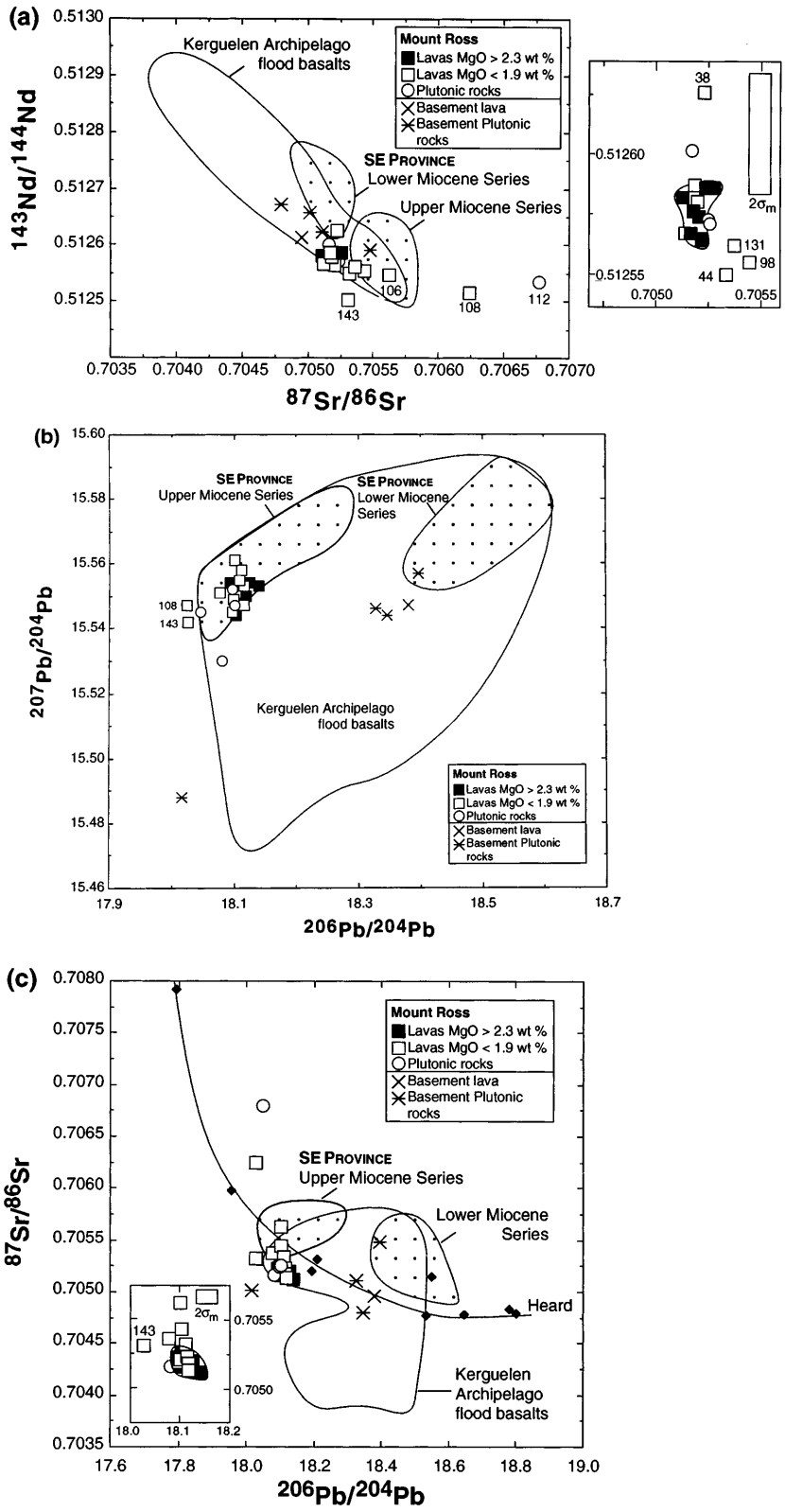
(a)
143Nd/144Nd
87Sr/86Sr
Kerguelen Archipelago flood basalts
Mount Ross
Lavas MgO > 2.3 wt %
Lavas MgO < 1.9 wt %
Plutonic rocks
Basement lava
Basement Plutonic rocks
SE Province
Lower Miocene Series
Upper Miocene Series
2σm
(b)
207Pb/204Pb
206Pb/204Pb
SE Province
Upper Miocene Series
SE Province
Lower Miocene Series
Kerguelen Archipelago flood basalts
(c)
87Sr/86Sr
206Pb/204Pb
SE Province
Upper Miocene Series
Lower Miocene Series
Heard
Kerguelen Archipelago flood basalts

Fig. 8.

contamination during the prolonged cooling and fractionation required to create highly evolved lavas. Of course, such contamination can only be recognized if the archipelago lithosphere is geochemically distinctive.

The subaerial Kerguelen Archipelago is on the northern part of the submarine Kerguelen Plateau (Fig. 1a). If this part of the plateau is Cretaceous and has a geochemically distinctive signature such as manifested in basalts from the southernmost Kerguelen Plateau and Eastern Broken Ridge (Mahoney *et al.*, 1995), it is likely that a component from the plateau lithosphere could be recognized in archipelago lavas. Although lavas from the southernmost Kerguelen Plateau and eastern Broken Ridge (Fig. 1a) have very distinctive abundance ratios of incompatible elements (e.g. Mahoney *et al.*, 1995), the use of such ratios to evaluate the role of assimilation in creating Mount Ross trachytes is not possible because many normally highly incompatible elements, such as P, REE, Nb and Ta, were affected by the apatite and Fe–Ti oxide fractionation required to create the evolved lavas (Figs 5 and 7). Therefore, isotopic ratios are more reliable indicators of assimilation of Kerguelen Plateau lithosphere. Except for alkalic basalt interbedded with sediment at ODP Site 748, all samples recovered from the submarine Kerguelen Plateau are tholeiitic basalts (Davies *et al.*, 1989; Weis *et al.*, 1989*a*; Storey *et al.*, 1992; Mahoney *et al.*, 1995). Relative to Mount Ross lavas, these tholeiitic basalts have lower abundances of Nd and Pb, but they have higher Sr contents (typically >200 ppm) than Mount Ross trachytes (190–7·7 ppm). Consequently, the $^{87}Sr/^{86}Sr$ of trachytic magmas are very sensitive to assimilation of Cretaceous lithosphere with very high $^{87}Sr/^{86}Sr$, such as recovered at ODP Site 738 (>0·7090) and on the eastern Broken Ridge (Mahoney *et al.*, 1995). Despite the complexity of significant age corrections for the high Rb/Sr trachytes (Table 3), eight of ten trachyandesites and trachytes, with MgO <1·9%, have initial $^{87}Sr/^{86}Sr$ within 3 SD of the field for the basaltic trachyandesites (Fig. 8a). None of these trachytes from Mount Ross show the high $^{87}Sr/^{86}Sr$ ratios observed in some Heard Island trachytes [Fig. 8c and Barling *et al.* (1994)]. Similarly, all of the evolved rocks have $^{143}Nd/^{144}Nd$ and 11 of the 13 have measured $^{206}Pb/^{204}Pb$ within 2 SD of the field for basaltic trachyandesites (Fig. 8).

Although most of the highly evolved lavas show little evidence for assimilation of isotopically distinct upper-crustal lithosphere, it is also possible that the more mafic archipelago lavas were affected by assimilation of lower crust and mantle lithosphere. We argue that the uniformity of isotopic ratios in magmas of varying composition erupted for 30 my is unlikely to be caused by lithosphere contamination. Moreover, most of the plutonic rocks of varying age (40 to <5 Ma) and composition (gabbro to nepheline syenite) exposed in the archipelago also have initial Sr, Nd and Pb isotopic ratios which overlap with the field for archipelago flood basalts (Weis & Giret, 1994) [initial $^{87}Sr/^{86}Sr$ in 50 of the 55 plutonic rocks ranges from 0·70425 to 0·70601—the five with higher ratios, to 0·73047, have very high $^{87}Rb/^{86}Sr$ (to 389) which may reflect high Rb contents created during hydrothermal alteration (Shaw, 1968)].

In summary, we conclude that there is no evidence in the Mount Ross lavas for assimilation of basalts with the continental-like signature of the Kerguelen Plateau basalts recovered from ODP Site 738. A possible interpretation is that, unlike the more southerly Heard Island (Fig. 1a), the Kerguelen Archipelago was not constructed on the Cretaceous part of the plateau (e.g. Coffin & Eldholm, 1994). However, a continental-like component is present in the mantle lithosphere below the archipelago. Several mantle xenoliths in archipelago lavas from the Courbet Peninsula have low Os isotopic ratios and one dunite xenolith from the Southeast Province has high $^{207}Pb/^{204}Pb$ (15·574) and very low $^{206}Pb/^{204}Pb$ (17·713); these isotopic data are interpreted as evidence for a continental component in the mantle lithosphere underlying the archipelago (Hassler & Shimizu, 1995; Mattielli *et al.*, 1996). The proportion of this continental component in the mantle is not known, but we do not find these isotopic features in archipelago lavas (Gautier *et al.*, 1990; Weis *et al.*, 1993; Yang *et al.*, 1998; and this paper); possible explanations are that these refractory dunite and harzburgite xenoliths cannot be easily assimilated or that this component is present only very locally as pieces of shredded continental lithosphere dispersed into the oceanic lithosphere during the break-up of Gondwana at >132 Ma.

## Implications for the geochemical characteristics of the Kerguelen plume

The debate about the isotopic characteristics of the Kerguelen plume has focused on the Upper Miocene lavas in the Southeast Province of the archipelago. Weis *et al.* (1993) argued that the isotopic ratios ($^{87}Sr/^{86}Sr$ = 0·7054–0·7058, $^{143}Nd/^{144}Nd$ = 0·51263–0·51249 and $^{206}Pb/^{204}Pb$ = 18·06–18·27) of these lavas are the 'purest' representation of the plume, whereas Class *et al.* (1996) argued that these lavas were significantly contaminated by the underlying Cretaceous(?) lithosphere that forms the Kerguelen Plateau. Frey & Weis (1996) discussed the complexities associated with identifying the isotopic characteristics of the Kerguelen plume, and they suggested that 'the best way to infer the geochemical characteristics of the Kerguelen plume is to utilize the temporal isotopic variations in lavas forming the Kerguelen Archipelago'. To date we have found that most of the 24–30 Ma flood basalts from three 0·5–1 km sections in the archipelago have initial $^{87}Sr/^{86}Sr$ >0·7050

and $^{143}Nd/^{144}Nd$ <0·5126 (Damasceno *et al.*, 1997; Yang *et al.*, 1998). These ratios for the oldest studied archipelago lavas overlap with those of the most mafic Mount Ross lavas, and they are offset from the field for Upper Miocene lavas to slightly lower $^{87}Sr/^{86}Sr$ (Fig. 8a and c). Because mafic lavas of diverse composition (transitional and alkalic basalt and basanite) and age (~30–0·1 Ma) have similar isotopic ratios, we continue to infer that archipelago lavas with relatively high $^{87}Sr/^{86}Sr$, low $^{143}Nd/^{144}Nd$ and low $^{206}Pb/^{204}Pb$ are representative of the Kerguelen plume. We acknowledge, however, that it is unlikely that the plume was isotopically homogeneous over the 115 my history of volcanism. Another aspect of the debate about the Kerguelen plume is whether the temporal isotopic variations of the plume-related lavas result from an evolving plume source (Class *et al.*, 1996; Frey & Weis, 1996). Mount Ross lavas, <1 Ma, and most of the oldest, 29–30 Ma, archipelago flood basalts analyzed are isotopically similar (Yang *et al.*, 1998); there is no evidence for an evolving plume source during the last ~30 my.

## SUMMARY

Mount Ross, the highest volcanic edifice in the Kerguelen Archipelago, is a <1 Ma Pleistocene volcano composed of a basaltic trachyandesite to trachyte lava series. Extensive glaciation has exposed a central plutonic complex ranging from gabbro to syenite. The compositional trends of the volcanic and plutonic rocks are qualitatively consistent with control by fractional crystallization. The absence of high MgO lavas and abundance of evolved lavas at Mount Ross and in the Southeast Province (Weis *et al.*, 1993) show that the magma supply to the archipelago has remained low for the last 20 my.

The most mafic Mount Ross rocks and most of the associated highly evolved rocks have a narrow range of isotopic ratios, initial $^{87}Sr/^{86}Sr$ from 0·70512 to 0·70532, $^{143}Nd/^{144}Nd$ from 0·51259 to 0·51250 and $^{206}Pb/^{204}Pb$ from 18·025 to 18·139. These ratios are close to the values proposed for the Kerguelen plume by Weis *et al.* (1993), and they overlap with those of the dominant basalt type forming the flood basalt in the northern and central part of the archipelago (Damasceno *et al.*, 1997; Yang *et al.*, 1998). A component with a continental geochemical signature has been found in some of the Cretaceous lavas forming the Kerguelen Plateau (Mahoney *et al.*, 1995) and in some trachytes on Heard Island (Barling *et al.*, 1994), and also in some xenoliths of lithospheric mantle found in archipelago lavas (Hassler & Shimizu, 1995; Mattielli *et al.*, 1996). However, there is no compelling evidence for this component in the compositions of Kerguelen archipelago lavas, not even in the highly evolved lavas which resided within the lithosphere for relatively long times.

## ACKNOWLEDGEMENTS

This work is part of the Kerguelen research program (D.W.: FNRS proposal 1.5.019.95F; F.A.F.: NSF proposal OPP-9417774 and EAR-9614532; A.G.: IFRTP, programme 'CARTOKER'). We thank the French IFRTP for the field support over the campaigns in 1986–1987, 1987–1988 and 1992–1993. D.W. thanks the FNRS for its financial support of her research and of the mass spectrometer analytical facilities. J. P. Mennessier is thanked for his help in the chemical processing of the samples, and P. Ila for supervision of the Neutron Activation Facility at MIT. D.W. and F.A.F. thank the Francqui Foundation for promoting collaboration between Belgian and US scientists. We thank M. C. Coffin for discussion, and W. Bohrson, C. Chauvel, C. Class, A. P. Le Roex, V. Salters and W. M. White for reviews.

## REFERENCES

Barling, J., Goldstein, S. L. & Nicholls, I. A. (1994). Geochemistry of Heard Island (Southern Indian Ocean): characterization of an enriched mantle component and implications for enrichment of the sub-Indian Ocean mantle. *Journal of Petrology* **35,** 1017–1053.

Blundy, J. D. & Wood, B. J. (1991). Crystal-chemical controls of Sr and Ba between plagioclase feldspar, silicate melts, and hydrothermal solutions. *Geochimica et Cosmochimica Acta* **55,** 193–207.

Boynton, W. V. (1984). Cosmochemistry of the rare earth elements: meteorite studies. In: Henderson, P. (ed.) *Rare Earth Element Geochemistry*. New York: Elsevier, pp. 63–114.

Cantagrel, J. M. & Baubron, J. C. (1983). Chronologie des éruptions dans le massif volcanique du Mont Dore (K–Ar). Implications volcanologiques. *Géologie de la France (2)* **1–2,** 123–142.

Class, C., Goldstein, S. L., Galer, S. G. & Weis, D. (1993). Young formation age of a mantle plume source. *Nature* **362,** 715–721.

Class, C., Goldstein, S. L. & Galer, S. J. G. (1996). Discussion of 'Temporal Evolution of the Kerguelen Plume: Geochemical Evidence from ~38 to 82 Ma Lavas Forming the Ninetyeast Ridge'. *Contributions to Mineralogy and Petrology* **124,** 98–103.

Coffin, M. F. & Eldholm, O. (1994). Large igneous provinces: crustal structure, dimensions, and external consequences. *Reviews of Geophysics* **32,** 1–36.

Damasceno, D., Scoates, J. S., Weis, D., Nicolaysen, K., Frey, F. A. & Giret, A. (1997). Phenocryst stratigraphy and geochemical variation in the Mount Crozier basaltic series, Kerguelen Archipelago: implications for the crystallization history of plume-related magmatism. *Terra Nova* **9,** 55.

Davies, H. L., Sun, S.-s., Frey, F. A., Gautier, I., McCulloch, M. T., Price, R. C., Bassias, Y., Klootwijk, C. T. & Leclaire, L. (1989). Basalt basement from the Kerguelen Plateau and the trail of a Dupal plume. *Contributions to Mineralogy and Petrology* **103,** 457–469.

Dosso, L., Vidal, P., Cantagrel, J. M., Lameyre, J., Marot, A. & Zimine, S. (1979). 'Kerguelen: continental fragment or oceanic island?'; petrology and isotopic geochemistry evidence. *Earth and Planetary Science Letters* **43,** 46–60.

Ellam, R. M. (1992). Lithospheric thickness as a control on basalt geochemistry. *Geology* **20,** 153–156.

Frey, F. A. & Weis, D. (1995). Geochemical constraints on the origin and evolution of the Ninetyeast Ridge: a 5000 km hotspot trace in the eastern Indian Ocean. *Contributions to Mineralogy and Petrology* **121,** 18–28.

Frey, F. A. & Weis, D. (1996). Reply to the Class *et al.* discussion of 'Temporal Evolution of the Kerguelen Plume: Geochemical Evidence from ~38 to 82 Ma Lavas Forming the Ninetyeast Ridge'. *Contributions to Mineralogy and Petrology* **124,** 104–110.

Frey, F. A., Jones, W. B., Davies, H. & Weis, D. (1991). Geochemical and petrologic data for basalts from Sites 756, 757, and 758: implications for the origin and evolution of Ninetyeast Ridge. In: Weissel, J., Peirce, J., Taylor, E., Alt, J., *et al.* (eds) *Proceedings of the Ocean Drilling Program, Scientific Results, 121*. College Station, TX: Ocean Drilling Program, pp. 611–659.

Gautier, I., Weis, D., Mennessier, J.-P., Vidal, P., Giret, A. & Loubet, M. (1990). Petrology and geochemistry of Kerguelen basalts (South Indian Ocean): evolution of the mantle sources from ridge to an intraplate position. *Earth and Planetary Science Letters* **100,** 59–76.

Giret, A. & Beaux, J.-F. (1984). The plutonic massif of Val Gabbro (Kerguelen Islands): a tholeiitic complex related to the activity of the East-Indian palaeoridge. *Comptes Rendus Hebdomadaires des Séances de l'Académie des Sciences* **299,** 965–969.

Giret, A. & Lameyre, J. (1983). A study of Kerguelen plutonism: petrology, geochronology and geological implications. In: Oliver, R. L., James, P. R. & Jago, J. B. *et al.* (eds) *Antarctic Earth Science*. Cambridge: Cambridge University Press, pp. 646–651.

Giret, A., Chotin, P. & Verdier, O. (1988). Des laves aux roches plutoniques. L'exemple du mont Ross, îles Kerguelen. *Comptes Rendus Hebdomadaires des Séances de l'Académie des Sciences* **306,** 381–386.

Hassler, D. & Shimizu, N. (1995). Old peridotite xenoliths from the Kerguelen Islands. *EOS Transactions, American Geophysical Union* **76,** F693–F694.

Ila, P. & Frey, F. A. (1984). Utilization of neutron activation analysis in the study of geologic materials. *Atomkernenergie Kerntechnik* **44,** 710–716.

Le Bas, M. J., Le Maître, R. W., Streickeisen, A. & Zanettin, B. (1986). A chemical classification of volcanic rocks based on the total alkali–silica diagram. *Journal of Petrology* **27,** 745–750.

le Roex, A. P. (1985). Geochemistry, mineralogy and magmatic evolution of the basaltic and trachytic lavas from Gough Island, South Atlantic. *Journal of Petrology* **26,** 149–186.

MacDonald, G. A. & Katsura, T. (1964). Chemical composition of Hawaiian lavas. *Journal of Petrology* **5,** 82–133.

Mahoney, J. J., Jones, W. B., Frey, F. A., Salters, V. J. M., Pyle, D. G. & Davies, H. L. (1995). Geochemical characteristics of lavas from Broken Ridge, the Naturaliste Plateau and southernmost Kerguelen plateau: Cretaceous plateau volcanism in the southeast Indian Ocean. *Chemical Geology* **120,** 315–345.

Mattielli, N., Weis, D., Mennessier, J. P., Shimizu, N., Cottin, J. Y., Grégoire, M. & Giret, A. (1996). Evidence for pervasive mantle metasomatism associated with the Kerguelen Plume. *EOS Transactions, American Geophysical Union* **77,** F827.

Nicolaysen, K., Frey, F. A., Hodges, K., Weis, D., Giret, A. & Leyrit, H. (1996). $^{40}Ar/^{39}Ar$ geochronology of flood basalts forming the Kerguelen Archipelago. *EOS Transactions, American Geophysical Union* **77,** F824.

Nougier, J. (1970). *Tomes I et II. Contribution à l'étude géologique et géomorphologique des Îles Kerguelen (Terres Australes et Antarctiques Françaises)*. Paris: CNFRA.

Recq, M., Le Roy, I., Charvis, P., Goslin, J. & Brefort, D. (1990). Structure profonde du Mont Ross d'après la réfraction sismique (Îles Kerguelen, Océan Indien austral). *Canadian Journal of Earth Sciences* **31,** 1806–1821.

Recq, M., Operto, S. & Charvis, P. (1994). Kerguelen Plateau: a hotspot related oceanic crust. *EOS Transactions, American Geophysical Union* **75,** 583.

Rhodes, J. M. (1983). Homogeneity of lava flows: chemical data for historical Mauna Loa eruptions. *Journal of Geophysical Research, Supplement* **88,** A869–A879.

Saunders, A. D., Storey, M., Kent, R. W. & Gibson, I. L. (1994). Magmatic activity associated with the Kerguelen–Heard plume: implications for plume dynamics. *Mémoires de la Société Géologique de France* **166,** 61–72.

Shaw, D. M. (1968). A review of K–Rb fractionation trends by covariance analysis. *Geochimica et Cosmochimica Acta* **32,** 573–601.

Spath, A., le Roex, A. P. & Duncan, R. A. (1996). The geochemistry of lavas from the Comores Archipelago, western Indian Ocean: petrogenesis and mantle source region characteristics. *Journal of Petrology* **37,** 961–991.

Storey, M., Saunders, A. D., Tarney, J., Leat, P., Thirlwall, M. F., Thompson, R. N., Menzies, M. A. & Marriner, G. F. (1988). Geochemical evidence for plume–mantle interactions beneath Kerguelen and Heard Islands, Indian Ocean. *Nature* **336,** 371–374.

Storey, M., Kent, R., Saunders, A. D., Salters, V. J., Hergt, J., Whitechurch, H., Sevigny, J. H., Thirwall, M. F., Leat, P., Ghose, N. C. & Gifford, M. (1992). Lower Cretaceous volcanic rocks along continental margins and their relationship to the Kerguelen Plateau. In: Wise, S. W., Jr & Schlich, R. (eds.) *Proceedings of the Ocean Drilling Program, Scientific Results, 120*. College Station, TX: Ocean Drilling Program, pp. 33–53.

Sun, S.-S. & McDonough, W. F. (1989). Chemical and isotopic systematics of oceanic basalts: implications for mantle composition and processes. In: Saunders, A. D. & Norry, M. J. (ed.) *Magmatism in the Ocean Basins. Special Publication, Geological Society, London* **42,** 313–345.

Swanson, D. A. (1972). Magma supply rate at Kilauea volcano. *Science* **175,** 169–170.

Watkins, N. D., Gunn, B. M., Nougier, J. & Baksi, A. K. (1974). Kerguelen: continental fragment or oceanic island. *Geological Society of America Bulletin* **85,** 201–212.

Watson, E. B. & Green, T. H. (1981). Apatite/liquid partition coefficients for rare earth elements and strontium. *Earth and Planetary Science Letters* **56,** 405–421.

Weaver, B. L. (1991). The origin of oceanic island basalt end-member compositions: trace element and isotopic constraints. *Earth and Planetary Science Letters* **104,** 381–397.

Weis, D. & Frey, F. A. (1991). Isotope geochemistry of Ninetyeast Ridge basalts: Sr, Nd, and Pb evidence for the involvement of the Kerguelen hot spot. In: Weissel, J., Peirce, J., Taylor, E., Alt, J., *et al.* (eds) *Proceedings of the Ocean Drilling Program, Scientific Results, 121*. College Station, TX: Ocean Drilling Program, pp. 591–610.

Weis, D. & Giret, A. (1994). Kerguelen plutonic complexes: Sr, Nd, Pb isotopic study and inferences about their sources, ages and geodynamic setting. *Bulletin de la Société Géologique de France* **166,** 47–59.

Weis, D., Demaiffe, D., Cauët, S. & Javoy, M. (1987). Sr, Nd, O and H isotopic ratios in Ascension Island lavas and plutonic inclusions: cogenetic origin. *Earth and Planetary Science Letters* **82,** 255–268.

Weis, D., Bassias, Y., Gautier, I. & Mennessier, J.-P. (1989*a*). Dupal anomaly in existence 115 Ma ago: evidence from isotopic study of the Kerguelen Plateau (South Indian Ocean). *Geochimica et Cosmochimica Acta* **53,** 2125–2131.

Weis, D., Beaux, J.-F., Gautier, I., Giret, A. & Vidal, P. (1989*b*). Kerguelen Archipelago: geochemical evidence for recycled material. In: Hart, S. R. & Gülen, L. (eds) *Crust/Mantle Recycling at Convergence Zones*. Dordrecht: Kluwer Academic, pp. 59–63.

Weis, D., White, W. M., Frey, F. A., Duncan, R. A., Dehn, J., Fisk,

M., Ludden, J., Saunders, A. & Storey, M. (1992). The influence of mantle plumes in generation of Indian Oceanic crust. In: Duncan, R. A., Rea, D. K., Kidd, R. B., von Rad, U. & Weissel, J. K. (eds.) *Synthesis of Results from the Scientific Drilling in the Indian Ocean*. Washington: American Geophyiscal Union, pp. 57–89.

Weis, D., Frey, F. A., Leyrit, H. & Gautier, I. (1993). Kerguelen Archipelago revisited: geochemical and isotopic study of the SE Province lavas. *Earth and Planetary Science Letters* **118,** 101–119.

Yang, Y. J., Frey, F. A., Nicolaysen, K., Weis, D. & Giret, A. (1998). Petrogenesis of flood basalts forming the Northern Kerguelen Archipelago: implications for the Kerguelen Plume. *Journal of Petrology* **39,** 711–748.